



HAL
open science

Optimal control of volume-preserving mean curvature flow

Antoine Laurain, Shawn W. Walker

► **To cite this version:**

Antoine Laurain, Shawn W. Walker. Optimal control of volume-preserving mean curvature flow. 2020. hal-02934959

HAL Id: hal-02934959

<https://hal.science/hal-02934959>

Preprint submitted on 9 Sep 2020

HAL is a multi-disciplinary open access archive for the deposit and dissemination of scientific research documents, whether they are published or not. The documents may come from teaching and research institutions in France or abroad, or from public or private research centers.

L'archive ouverte pluridisciplinaire **HAL**, est destinée au dépôt et à la diffusion de documents scientifiques de niveau recherche, publiés ou non, émanant des établissements d'enseignement et de recherche français ou étrangers, des laboratoires publics ou privés.

Optimal control of volume-preserving mean curvature flow

Antoine Laurain

Department of Applied Mathematics
Universidade de São Paulo
Email: laurain@ime.usp.br

Shawn W. Walker

Department of Mathematics
Louisiana State University,
Baton Rouge, LA 70803-4918, U.S.A.
Email: walker@math.lsu.edu

Abstract

We develop a framework and numerical method for controlling the full space-time tube of a geometrically driven flow. We consider an optimal control problem for the mean curvature flow of a curve or surface with a volume constraint, where the control parameter acts as a forcing term in the motion law. The control of the trajectory of the flow is achieved by minimizing an appropriate tracking-type cost functional. The gradient of the cost functional is obtained via a formal sensitivity analysis of the space-time tube generated by the mean curvature flow. We show that the perturbation of the tube may be described by a transverse field satisfying a parabolic equation on the tube. We propose a numerical algorithm to approximate the optimal control and show several results in two and three dimensions demonstrating the efficiency of the approach.

Keywords: mean curvature flow, optimal control, transverse field, PDEs on moving surfaces

1 Introduction

There exists a host of applications that involve large deformations or geometric flows: the motion of droplets [21], fluid structure interaction [22, 6], mean curvature flow [3, 14, 18], deformable elastic bodies [31, 34, 37], liquid thin films on curved surfaces [32] to name a few. Such problems can often be formulated as the evolution of sets under a gradient flow. A simple yet challenging example of gradient flow is the evolution by mean curvature flow (MCF), for which a rich mathematical theory has been developed. The main focus of the literature on MCF is the proof of existence and regularity of the flow, and the study of its geometric properties.

Controlling these complex motions can further extend these applications or make them more optimal. However, this question has not been addressed yet except for the theoretical work of Zolésio and his collaborators; see [13, 24]. Moreover, the numerical realization of optimal geometric control is sorely lacking. The optimal control of gradient flows is of course a challenging topic, considering for instance that even the MCF is still a very active field of research with many open questions.

In this paper, we consider an optimal control problem for the mean curvature flow of a curve or surface (embedded manifold) with a volume constraint on the evolving domain. The goal is to control the evolution of the manifold so that it tracks a desired trajectory; this is accomplished by introducing an appropriate control variable into the motion law of the manifold. Thus, our problem

can be seen as the optimal control of a volume-preserving MCF with a forcing term. We note that there exists an extensive literature on volume-preserving MCF, see the regularized mean curvature flow of [20] and also [3, 19], and on MCF with forcing term, see [10, 18, 19].

The control of the trajectory of the evolving set may be formulated as the control of the *space-time tube* defined by this evolving set. We seek to solve a time-dependent geometric PDE constrained optimization problem to minimize an appropriate tracking-type functional. The desired trajectory is determined by the zero level set of a given function. The theoretical study of the optimal control of such space-time tubes has been pioneered by Zolésio and its collaborators; see [13, 24]. Using the concept of *transverse field*, they performed the sensitivity analysis of the flow with respect to perturbations of the motion law. This concept of transverse field plays a key role in our approach.

The main task in our framework is to relate the perturbation of the control, which appears as a forcing term in the motion law, with the perturbation of the motion law. Compared to the theory and applications developed in [13, 24], we are facing an additional fundamental difficulty. Indeed in our problem the motion law is implicitly defined as it depends on the shape of the space-time tube via the mean curvature term. We tackle this issue using a formal perturbation analysis of the flow. In this way we are able to show that the perturbation of the flow can be described by a parabolic PDE on the space-time tube generated by the flow. This allows us to compute the derivative of the tracking-type functional with respect to the control, via the introduction of an appropriate adjoint state.

The type of problem considered in this paper shares many similarities with the optimal control of free boundaries for stationary problems. Recent contributions on this topic have been obtained using tools from shape calculus including [16, 33] for the shape controllability of the free boundary of an obstacle problem, [17] where the control of the Bernoulli free boundary problem has been investigated, and [21] for the control of the footprint of a sessile droplet via substrate surface tension. In these works, the free boundary depends implicitly on the control and a perturbation analysis allows to compute the sensitivity of the free boundary with respect to the control. The problem considered in the present paper is similar in the sense that the space-time tube also depends implicitly on the control. Thus, on one hand several ideas of [17, 21] may be used, but on the other hand the control of the geometric evolution problem presents many specificities that require a different analysis and novel ideas. To the best of our knowledge this is the first investigation of optimal control of geometric evolution problems and MCF.

The paper is organized as follows. In Section 2 we introduce the volume-preserving MCF with forcing term and describe the optimal control problem via the minimization of a tracking-type cost functional. In Section 3 we perform the sensitivity analysis of the cost functional with respect to a small perturbation of the control and obtain the gradient of the cost functional via the introduction of an adjoint transverse field. We also show an alternative expression of the gradient of the cost functional based on a scalar adjoint. In Section 4 we explain the optimization scheme and its discretization. Section 5 presents numerical results in two and three dimensions. We conclude with some remarks in Section 6.

2 Control of the mean curvature flow

2.1 Volume-preserving mean curvature flow with forcing term

Let $\mathfrak{D} \subset \mathbb{R}^n$ be a bounded open set which contains all admissible domains for our problem. We consider vector fields with compact support in \mathfrak{D} , satisfying

$$\mathcal{V} := \mathcal{C}([0, t_f]; \mathcal{C}_c^\infty(\mathfrak{D}, \mathbb{R}^n)), \quad (1)$$

where $t_f > 0$ denotes the final time for our interval of interest $[0, t_f]$. For a given $\mathbf{V} \in \mathcal{V}$ and $\mathbf{x}^0 \in \mathfrak{D}$, let $\mathbf{x}(t)$ be the solution of

$$\begin{aligned}\dot{\mathbf{x}}(t) &= \mathbf{V}(t, \mathbf{x}(t)), & \text{for } t \in [0, t_f], \\ \mathbf{x}(0) &= \mathbf{x}^0.\end{aligned}\tag{2}$$

Thus, for all $t \in [0, t_f]$, we can define a transformation $T^t(\mathbf{V}) : \overline{\mathfrak{D}} \rightarrow \overline{\mathfrak{D}}$ by $T^t(\mathbf{V})(\mathbf{x}^0) := \mathbf{x}(t)$.

Next, let $\Gamma \subset \mathfrak{D}$ be a smooth $(n-1)$ -dimensional embedded manifold, without boundary, whose interior is Ω , i.e. $\Gamma \equiv \partial\Omega$. For $t \in [0, t_f]$, let us consider formally the evolution of sets $\Gamma^t = \Gamma^t(\mathbf{V})$ given by the following motion law

$$\mathbf{V}|_{\Gamma^t} = (u|_{\Gamma^t} - \kappa(t) - \lambda(t))\boldsymbol{\nu}(t) \quad \text{for } t \in [0, t_f],\tag{3}$$

where $\boldsymbol{\nu}(t)$ is the outer normal vector of Γ^t , $\kappa(t)$ is the (additive) curvature of $\Gamma^t(\mathbf{V})$, $\lambda(t)$ is a Lagrange multiplier to enforce the constraint that $|\Omega^t|$ is constant for all $t \in [0, t_f]$, where Ω^t is the interior of Γ^t (i.e. $\Gamma^t \equiv \partial\Omega^t$), and $u \in \mathcal{C}^\infty(\mathfrak{D})$ is a given control function. The motion law (3) can be described as a volume-preserving MCF with a forcing term u , and \mathbf{V} can be derived from a gradient flow with a volume constraint; see [3]. Indeed, \mathbf{V} is the (volume-preserving) L^2 -gradient flow of the ‘‘energy’’

$$\mathcal{E}[\Omega] = \int_{\Gamma} 1 - \int_{\Omega} u.\tag{4}$$

Note that (3) is an implicit definition of \mathbf{V} since κ, λ and $\boldsymbol{\nu}$ depend on \mathbf{V} through $\Gamma^t(\mathbf{V})$. The existence of the evolution of sets $\Gamma^t(\mathbf{V})$ may be proven in the sense of viscosity solutions; see [7, 14]. This approach allows topological changes, but the drawback is that fattening of $\Gamma^t(\mathbf{V})$ can occur. Another approach is to use parameterization, this avoids the fattening phenomenon but in this case singularities may appear in finite time. In two dimensions, i.e. when $\Gamma^t(\mathbf{V})$ is a curve, a more precise analysis is given in [4, 5], but singularity may still appear; see [23]. In any case, finite-time singularities can be expected with the motion law (3).

In this paper we assume existence and smoothness of the sets $\Gamma^t(\mathbf{V})$ for $t \in [0, t_f]$ under the motion law (3), and define the smooth transformation $T^t(\mathbf{V})(\Gamma) := \Gamma^t(\mathbf{V})$. We also assume that $\boldsymbol{\nu}$ and κ can be extended so that $\mathbf{V}|_{\Gamma^t}$ can be extended to all of \mathfrak{D} and that $\mathbf{V} = \mathbf{V}(u) \in \mathcal{V}$.

2.2 Tracking-type cost functional

Our objective is to determine a control u in (3) such that the evolution of sets $\Gamma^t(\mathbf{V})$ is as close as possible to a given target trajectory. A convenient way to achieve this is to minimize a tracking-type functional based on a level set function. Let $\phi : [0, t_f] \times \mathfrak{D} \rightarrow \mathbb{R}$ be a given smooth function and define its sublevel set

$$Q_d := \{(t, \mathbf{x}) \in [0, t_f] \times \mathfrak{D} \mid \phi(t, \mathbf{x}) < 0\}.\tag{5}$$

Then Q_d is called the *target trajectory*. Next, introduce the tracking-type cost functional

$$J(\mathbf{V}(u)) := \int_0^{t_f} \int_{\Omega^t(\mathbf{V}(u))} \phi,\tag{6}$$

and the *reduced* functional, including a Tikhonov regularization of the control,

$$\mathcal{J}(u) := J(\mathbf{V}(u)) + \frac{\alpha}{2} \|\nabla u\|_{L^2(\mathfrak{D})}^2.$$

Consider the minimization problem

$$\text{minimize } \mathcal{J}(u), \quad \text{subject to } u \in \mathcal{C}^\infty(\mathfrak{D}). \quad (7)$$

To understand the relevance of the minimization problem (7) to achieve the control objective, we need to introduce the notion of *tubes*.

Definition 1. For a set $\mathcal{A} \subset \mathbb{R}^n$, let the space-time \mathcal{A} -tube be given by

$$Q_{\mathcal{A}}(\mathbf{V}) := \bigcup_{0 \leq t \leq t_f} \{t\} \times T^t(\mathbf{V})(\mathcal{A}). \quad (8)$$

In view of (5) and (6), if there exists a control $u \in \mathcal{C}^\infty(\mathfrak{D})$ such that $Q_\Omega(\mathbf{V}(u)) = Q_d$, then the minimum of $J(\mathbf{V}(u))$ is attained precisely for this control. The Tikhonov regularization in $\mathcal{J}(u)$ allows to find a compromise between reaching the target Q_d and obtaining a smooth control u .

3 Derivative of the cost functional

To devise a numerical algorithm to find an approximate solution of (7), the gradient of $\mathcal{J}(u)$ needs to be computed. Two main difficulties arise when considering this computation. The first one is the dependence of Ω^t on \mathbf{V} in (6). This dependence is relatively well-understood and can be handled via the concept of *transverse field* introduced in [13, 24]. The second difficulty comes from the fact that the motion law (3) is an implicit definition of \mathbf{V} . This makes the sensitivity analysis of \mathbf{V} with respect to u challenging, since a small perturbation of u induces a perturbation of \mathbf{V} not only through equation (3) but also through the variation of Γ^t . Such a difficulty is new in the area of control of geometric evolution equations, but we may borrow certain ideas from optimal control of free boundary problems [17, 21] to tackle this issue.

3.1 Derivative of tube functionals via transverse field

In [13, 24] the sensitivity analysis of cost functionals $J(\mathbf{V})$ of the type (6), sometimes called tube functionals, with respect to variations of \mathbf{V} has been investigated. The chief ingredient to compute the derivative of such cost functionals with respect to \mathbf{V} is the concept of *transverse field* (see Figure 1). We briefly explain here how this concept can be applied to our problem.

Let $\mathbf{V}, \mathbf{W} \in \mathcal{V}$ and consider the tube $Q_\Omega(\mathbf{V})$, see Definition 1. Let $T_r^t : \overline{\mathfrak{D}} \rightarrow \overline{\mathfrak{D}}$ be the transformation generated by the time varying field $\mathbf{V}(t, \cdot) + s\mathbf{W}(t, \cdot)$, with $T_0^t = T^t$. The perturbed moving set is denoted by $\Omega_s^t := T_s^t(\Omega)$. The following expression for the derivative of $J(\mathbf{V})$ with respect to $\mathbf{W} \in \mathcal{V}$ may be found in [24, Section 3.4.1], see also [13]:

$$[\delta J(\mathbf{V})](\mathbf{W}) = \int_0^{t_f} \int_{\Gamma^t(\mathbf{V})} \phi(t, \mathbf{x}) \mathbf{Z}(t, \mathbf{x}) \cdot \boldsymbol{\nu}(t, \mathbf{x}), \quad (9)$$

where $\mathbf{Z} : [0, t_f] \times \mathfrak{D} \rightarrow \mathbb{R}^n$ is the so-called *transverse field*, which depends on \mathbf{W} in the following way:

$$\begin{aligned} \partial_t \mathbf{Z} + [\mathbf{Z}, \mathbf{V}] &= \mathbf{W}, \quad \text{in } (0, t_f) \times \mathfrak{D}, \\ \mathbf{Z}(0, \cdot) &= \mathbf{0}, \quad \text{in } \mathfrak{D}, \end{aligned} \quad (10)$$

where $[\cdot, \cdot]$ denotes the Lie bracket, i.e. $[\mathbf{Z}, \mathbf{V}] := (D\mathbf{Z})\mathbf{V} - (D\mathbf{V})\mathbf{Z}$. We introduce the notion of material derivative to clarify the question of the solvability of (10).

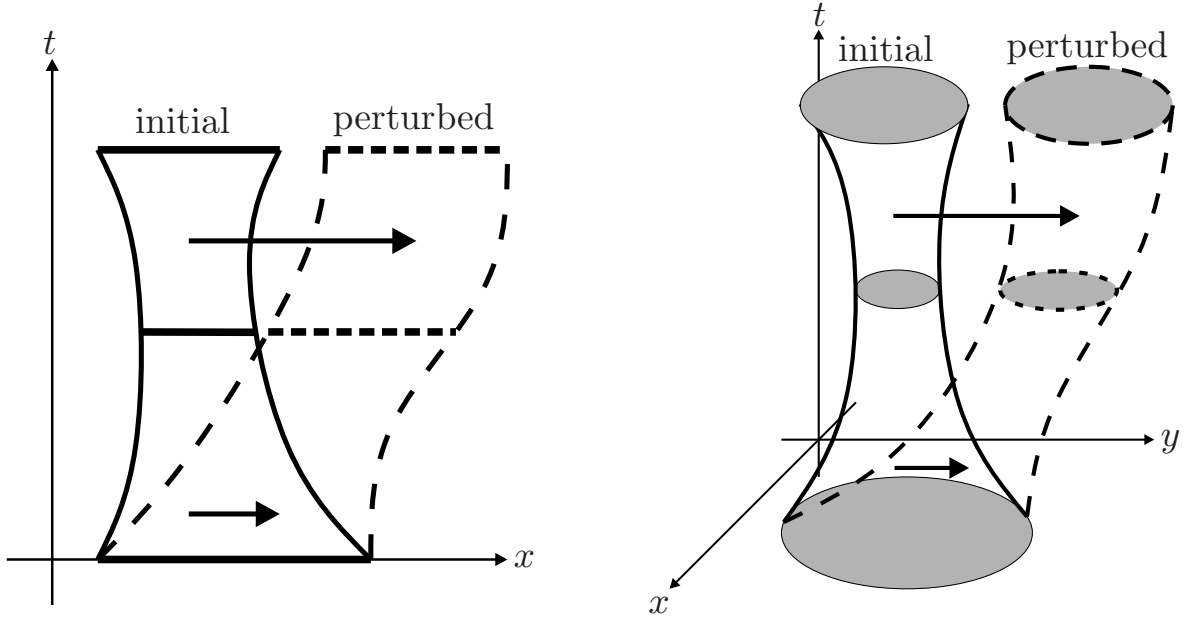


Figure 1: Diagram of the space-time tube for one dimensional domains (left) and two dimensional domains (right). The time axis is vertical. The initial tube corresponds to $Q_\Omega(\mathbf{V})$, while the perturbed tube corresponds to $Q_\Omega(\mathbf{V} + s\mathbf{W})$; see Definition 8. The transverse field \mathbf{Z} is indicated by the arrows and corresponds to $\partial_s T_s^t(\Omega)|_{s=0}$.

Definition 2 (Material Derivative). *Let $f : (0, t_f) \times \mathfrak{D} \rightarrow \mathbb{R}$ be \mathcal{C}^1 , and let $\mathbf{V} : \mathfrak{D} \rightarrow \mathbb{R}^n$ be a continuous velocity field. Then, we define the material derivative of f as*

$$D_{\mathbf{V}} f \circ T^t(\mathbf{V}) := \frac{d}{dt}[f \circ T^t(\mathbf{V})].$$

The material derivative for functions defined on subsets of \mathfrak{D} and the material derivative of vector-valued functions are defined in a similar way.

Thus, $\partial_t \mathbf{Z} + (D\mathbf{Z})\mathbf{V} \equiv D_{\mathbf{V}} \mathbf{Z}$ and the first line of (10) is simply $D_{\mathbf{V}} \mathbf{Z} - (D\mathbf{V})\mathbf{Z} = \mathbf{W}$. Indeed, if $\mathbf{x}(t)$ is the trajectory of a point driven by \mathbf{V} , then (10) is simply an ordinary differential equation (ODE), i.e. $\mathbf{Z}(\mathbf{x}(t))' - (D\mathbf{V}(\mathbf{x}(t)))\mathbf{Z}(\mathbf{x}(t)) = \mathbf{W}(\mathbf{x}(t))$, whose solvability is guaranteed by the theory of ODEs. Solving the ODE for every possible trajectory yields the unique solution of (10), see [24].

We also recall the concept of shape derivative which is a convenient tool for the forthcoming calculations. We refer to [35, Section 5.4] and [12, 15, 33] for more details on the notions of material and shape derivatives.

Definition 3 (Shape Derivative). *Let $f : (0, t_f) \times \mathfrak{D} \rightarrow \mathbb{R}^n$ be \mathcal{C}^1 , and let $\mathbf{V} : \mathfrak{D} \rightarrow \mathbb{R}^n$ be a continuous velocity field. Then, we define the shape derivative of f as*

$$\delta_\Omega f(\mathbf{V}) := [D_{\mathbf{V}} f - \mathbf{V} \cdot \nabla f]|_{t=0}.$$

The shape derivative for functions defined on subsets of \mathfrak{D} and the shape derivative of vector-valued functions is defined in a similar way.

3.2 Sensitivity analysis of the tube with respect to the control

Considering $J(\mathbf{V}(u))$ of (6) as the composition of functions $u \mapsto \mathbf{V}(u)$ and $\mathbf{V} \mapsto J(\mathbf{V})$, we have seen that the differentiability of $\mathbf{V} \mapsto J(\mathbf{V})$ can be handled via the notion of transverse field in Section

3.1. The differentiability of $u \mapsto \mathbf{V}(u)$ on the other hand is a delicate issue since \mathbf{V} also depends on $\Gamma^t(\mathbf{V})$. Here we perform a formal sensitivity analysis of $u \mapsto \mathbf{V}(u)$, borrowing some ideas from [17, 21].

Let $\eta \in \mathcal{C}^\infty(\mathfrak{D})$ and consider the following perturbation of the control

$$u_\epsilon := u + \epsilon\eta. \quad (11)$$

The main idea of the sensitivity analysis can be summarized in the following way. The first-order perturbation of $J(\mathbf{V}(u))$ with respect to the control u can also be described via the transverse field equation (10), except that the vector \mathbf{W} appearing in (10) also depends on \mathbf{Z} and η in this case. This provides a new transverse field equation involving only \mathbf{Z} and η . Hence, our main task is to determine the dependence of \mathbf{W} on \mathbf{Z} and η .

In view of the motion law (3), the corresponding perturbed sets $\Gamma^t(\mathbf{V}(u_\epsilon))$ and perturbed vector field satisfy

$$\mathbf{V}(u_\epsilon) = ((u + \epsilon\eta)|_{\Gamma^t(\mathbf{V}(u_\epsilon))} - \kappa(\epsilon) - \lambda(\epsilon))\boldsymbol{\nu}(\epsilon) \quad \text{on } \Gamma^t(\mathbf{V}(u_\epsilon)), \quad (12)$$

where $\boldsymbol{\nu}(\epsilon)$, $\kappa(\epsilon)$ and $\lambda(\epsilon)$ are the corresponding normal vector, curvature and Lagrange multiplier, respectively. The perturbed cost functional $\mathcal{J}(u_\epsilon)$ is defined accordingly and we also define the interior $\Omega^t(\mathbf{V}(u_\epsilon))$ of $\Gamma^t(\mathbf{V}(u_\epsilon))$. We need to extend $\mathbf{V}(u_\epsilon)$ to a neighborhood of $\Gamma^t(\mathbf{V}(u_\epsilon))$ since u is defined on all of \mathfrak{D} and not just on the boundary $\Gamma^t(\mathbf{V}(u_\epsilon))$. To define such an extension, we first use a unitary extension of $\boldsymbol{\nu}$ along $\boldsymbol{\nu}$, which in turn induces an extension of κ (not necessarily constant along the normal direction $\boldsymbol{\nu}$). With such an extension, it is known that the shape derivative of κ in a direction \mathbf{Y} (see Definition 3) is given by

$$\delta_\Omega \kappa(\mathbf{Y}) = -\Delta_\Gamma(\mathbf{Y} \cdot \boldsymbol{\nu}), \quad (13)$$

where Δ_Γ denotes the Laplace-Beltrami operator on $\Gamma^t(\mathbf{V}(u))$; see [35, lemma 5.6], [21, p. 783] or [11].

We now explain the main idea of the sensitivity analysis. Let us assume that there exists a smooth transformation $\mathcal{T}_\epsilon^t : \overline{\mathfrak{D}} \rightarrow \overline{\mathfrak{D}}$ such that $\mathcal{T}_\epsilon^t(\Gamma^t(\mathbf{V}(u))) = \Gamma^t(\mathbf{V}(u_\epsilon))$. In order to perform the sensitivity analysis of $\mathbf{V}(u_\epsilon)$, we suppose that $\mathbf{V}(u_\epsilon)$ has the form $\mathbf{V}(u_\epsilon) \circ \mathcal{T}_\epsilon^t = \mathbf{V}(u) + \widetilde{\mathbf{W}}(\epsilon)$ on $\Gamma^t(\mathbf{V}(u))$, where $\widetilde{\mathbf{W}}(\epsilon) \in \mathcal{V}$ with $\widetilde{\mathbf{W}}(0) = \mathbf{0}$. Assuming $\widetilde{\mathbf{W}}(\epsilon)$ is sufficiently smooth with respect to ϵ , we have the expansion $\widetilde{\mathbf{W}}(\epsilon) = \epsilon\widetilde{\mathbf{W}}'(0) + O(\epsilon^2)$. The computation of the derivative of $\epsilon \mapsto \mathcal{J}(u_\epsilon)$ at $\epsilon = 0$ only requires to know $\widetilde{\mathbf{W}}'(0)$ instead of $\widetilde{\mathbf{W}}(\epsilon)$; a similar idea was used in [21]. Thus we introduce the notation $\mathbf{W} := \widetilde{\mathbf{W}}'(0)$ and in what follows we proceed to determine \mathbf{W} as a function of the transverse field \mathbf{Z} and η . Combining this with the transverse field equation (10) one obtains an equation involving only \mathbf{Z} and η .

Next, we identify the equation for \mathbf{W} by considering the weak formulation of the perturbed gradient flow (12):

$$I(\epsilon) := \int_0^{t_f} \int_{\Gamma^t(\mathbf{V}(u_\epsilon))} [\mathbf{V}(u_\epsilon) - (u + \epsilon\eta - \kappa(\epsilon) - \lambda(\epsilon))\boldsymbol{\nu}(\epsilon)] \cdot \boldsymbol{\xi} = 0, \quad \forall \boldsymbol{\xi} \in \mathcal{V}, \quad (14)$$

with the volume constraint

$$\int_0^{t_f} \mu(t) (|\Omega^t(\mathbf{V}(u_\epsilon))| - C_V) dt = 0, \quad \forall \mu \in L^1([0, t_f]), \quad (15)$$

for some fixed volume constant C_V . Note that μ is independent of ϵ .

Since $\kappa(\epsilon)$, $\lambda(\epsilon)$ and $\boldsymbol{\nu}(\epsilon)$ correspond to the perturbation $\mathbf{V}(u_\epsilon) \circ \mathcal{T}_\epsilon^t = \mathbf{V}(u) + \widetilde{\mathbf{W}}(\epsilon)$, then the results of [13, 24] show that the derivatives with respect to ϵ of $\kappa(\epsilon)$, $\lambda(\epsilon)$ and $\boldsymbol{\nu}(\epsilon)$ at $\epsilon = 0$ are equal

to the shape derivatives of these quantities with respect to the transverse field \mathbf{Z} , given by (10), corresponding to the perturbation $\mathbf{V}(u_\epsilon)$. For instance we have

$$\boldsymbol{\nu}'(0) = \left. \frac{d\boldsymbol{\nu}(\epsilon)}{d\epsilon} \right|_{t=0} = \delta_\Omega \boldsymbol{\nu}(\mathbf{Z}).$$

Since we have assumed a unitary extension of $\boldsymbol{\nu}$ along the normal $\boldsymbol{\nu}$ it is known that $\delta_\Omega \boldsymbol{\nu}(\mathbf{Z}) = -\nabla_\Gamma(\mathbf{Z} \cdot \boldsymbol{\nu})$; see [35, lemma 5.5] or [15, Proposition 5.4.14]. Therefore we have

$$\boldsymbol{\nu}'(0) = -\nabla_\Gamma(\mathbf{Z} \cdot \boldsymbol{\nu}). \quad (16)$$

Furthermore, in view of (13) the derivative of $\kappa(\epsilon)$ is given by

$$\kappa'(0) = -\Delta_\Gamma(\mathbf{Z} \cdot \boldsymbol{\nu}). \quad (17)$$

Let us recall a general formula for the shape derivative of a boundary integral, see for instance [12, Theorem 4.3, Chapter 9] or [35, Eqn. (5.48)]. For a smooth transformation $T^\epsilon(\mathbf{Y}) : \overline{\mathfrak{D}} \rightarrow \overline{\mathfrak{D}}$, a smooth $(n-1)$ -dimensional embedded manifold γ and a sufficiently smooth function f , we have

$$\left. \frac{d}{d\epsilon} \int_{T^\epsilon(\mathbf{Y})(\gamma)} f(\epsilon, \mathbf{x}) dS(\mathbf{x}) \right|_{\epsilon=0} = \int_\gamma \partial_\epsilon f(0, \mathbf{x}) + (\partial_\nu f(0, \mathbf{x}) + f(0, \mathbf{x})\kappa)(\mathbf{Y} \cdot \boldsymbol{\nu}) dS(\mathbf{x}). \quad (18)$$

Using (16), (17) and (18) we can now compute the derivative of (14) as

$$\begin{aligned} I'(0) &= \int_0^{t_f} \int_{\Gamma^t(\mathbf{V}(u))} [\mathbf{W} - (\eta + \Delta_\Gamma(\mathbf{Z} \cdot \boldsymbol{\nu}) - \lambda'(0))\boldsymbol{\nu} + (u - \kappa - \lambda)\nabla_\Gamma(\mathbf{Z} \cdot \boldsymbol{\nu})] \cdot \boldsymbol{\xi} \\ &\quad + \int_0^{t_f} \int_{\Gamma^t(\mathbf{V}(u))} \left(\partial_\nu([\mathbf{V} - (u - \kappa - \lambda)\boldsymbol{\nu}] \cdot \boldsymbol{\xi}) + \underbrace{\kappa[\mathbf{V} - (u - \kappa - \lambda)\boldsymbol{\nu}] \cdot \boldsymbol{\xi}}_{=0} \right) (\mathbf{Z} \cdot \boldsymbol{\nu}). \end{aligned}$$

Note that we have

$$\begin{aligned} \partial_\nu([\mathbf{V} - (u - \kappa - \lambda)\boldsymbol{\nu}] \cdot \boldsymbol{\xi}) &= D([\mathbf{V} - (u - \kappa - \lambda)\boldsymbol{\nu}] \cdot \boldsymbol{\xi}) \cdot \boldsymbol{\nu} \\ &= D[\mathbf{V} - (u - \kappa - \lambda)\boldsymbol{\nu}] \boldsymbol{\nu} \cdot \boldsymbol{\xi} + (D\boldsymbol{\xi}) \boldsymbol{\nu} \cdot \underbrace{[\mathbf{V} - (u - \kappa - \lambda)\boldsymbol{\nu}]}_{=0} \\ &= D[\mathbf{V} - (u - \kappa - \lambda)\boldsymbol{\nu}] \boldsymbol{\nu} \cdot \boldsymbol{\xi}. \end{aligned}$$

Introducing the time-varying, spatial constant $\rho := \lambda'(0)$, we obtain for all $\boldsymbol{\xi} \in \mathcal{V}$:

$$\begin{aligned} 0 = I'(0) &= \int_0^{t_f} \int_{\Gamma^t(\mathbf{V}(u))} [\mathbf{W} - (\eta + \Delta_\Gamma(\mathbf{Z} \cdot \boldsymbol{\nu}) - \rho)\boldsymbol{\nu} + (u - \kappa - \lambda)\nabla_\Gamma(\mathbf{Z} \cdot \boldsymbol{\nu})] \cdot \boldsymbol{\xi} \\ &\quad + \int_0^{t_f} \int_{\Gamma^t(\mathbf{V}(u))} D[\mathbf{V} - (u - \kappa - \lambda)\boldsymbol{\nu}] \boldsymbol{\nu} \cdot \boldsymbol{\xi} (\mathbf{Z} \cdot \boldsymbol{\nu}). \end{aligned}$$

In fact we also have $D[\mathbf{V} - (u - \kappa - \lambda)\boldsymbol{\nu}] = 0$ on $\Gamma^t(\mathbf{V}(u))$ due to $\mathbf{V} = (u - \kappa - \lambda)\boldsymbol{\nu}$ in a neighborhood of $\Gamma^t(\mathbf{V}(u))$. Furthermore, differentiating (15) yields

$$\int_0^{t_f} \mu(t) \int_{\Gamma^t(\mathbf{V}(u))} \mathbf{Z}(t, \mathbf{x}) \cdot \boldsymbol{\nu}(t, \mathbf{x}) = 0, \quad \forall \mu \in L^1([0, t_f]). \quad (19)$$

Hence, we arrive at the following equations relating \mathbf{W} , ρ and \mathbf{Z} on Γ^t :

$$[\mathbf{W} - (\eta + \Delta_\Gamma(\mathbf{Z} \cdot \boldsymbol{\nu}) - \rho)\boldsymbol{\nu} + (u - \kappa - \lambda)\nabla_\Gamma(\mathbf{Z} \cdot \boldsymbol{\nu})] = \mathbf{0} \quad \text{on } \Gamma^t(\mathbf{V}(u)), \quad (20)$$

$$\int_{\Gamma^t(\mathbf{V}(u))} \mathbf{Z}(t, \mathbf{x}) \cdot \boldsymbol{\nu}(t, \mathbf{x}) = 0. \quad (21)$$

Note that ρ plays the role of a Lagrange multiplier for the volume constraint (21).

The transverse field \mathbf{Z} and the perturbation field \mathbf{W} are also related by equation (10). Thus, combining (10) and (20)-(21) yields the new transverse field equation for \mathbf{Z} . However, (20) shows that $\mathbf{W}|_{\Gamma^t}$ only depends on the values of \mathbf{Z} on Γ^t , but we need \mathbf{W} defined on \mathfrak{D} in order to use (10). Hence, we assume \mathbf{W} can be extended from Γ^t to all of \mathfrak{D} in a smooth way, and then we may *restrict* (10) to Γ^t . We obtain the following system of equations for \mathbf{Z} :

$$\begin{aligned} \partial_t \mathbf{Z} + (D\mathbf{Z})\mathbf{V} + A\mathbf{Z} + \rho\boldsymbol{\nu} &= \eta\boldsymbol{\nu}, \quad \text{on } \Gamma^t(\mathbf{V}(u)) \text{ for all } t \in (0, t_f), \\ \int_{\Gamma^t(\mathbf{V}(u))} \mathbf{Z}(t, \mathbf{x}) \cdot \boldsymbol{\nu}(t, \mathbf{x}) &= 0, \quad \text{for all } t \in (0, t_f), \\ \mathbf{Z}(0, \cdot) &= \mathbf{0}, \quad \text{on } \Gamma^0(\mathbf{V}(u)), \end{aligned} \quad (22)$$

where the state operator A is given by

$$A\mathbf{Z} := -(D\mathbf{V})\mathbf{Z} - \Delta_\Gamma(\mathbf{Z} \cdot \boldsymbol{\nu})\boldsymbol{\nu} + (u - \kappa - \lambda)\nabla_\Gamma(\mathbf{Z} \cdot \boldsymbol{\nu}) \quad \text{on } \Gamma^t(\mathbf{V}(u)). \quad (23)$$

Note that $A\mathbf{Z}$ only depends on the values of \mathbf{Z} on Γ^t . Also, the material derivative $D_{\mathbf{V}}\mathbf{Z} := \partial_t \mathbf{Z} + (D\mathbf{Z})\mathbf{V}$ is *independent* of any extension of \mathbf{Z} even though the constitutive terms are not, i.e. $\partial_t \mathbf{Z}$ and $(D\mathbf{Z})\mathbf{V}$ do depend on the extension. Hence, (22) fully describes the evolution of \mathbf{Z} on Γ^t , in the sense that it is independent of the values of \mathbf{Z} outside of Γ^t .

3.3 Derivative of the cost functional and adjoint transverse field

We can now compute the derivative of $u \mapsto J(\mathbf{V}(u))$ by formally applying the chain rule to the composition of functions $u \mapsto \mathbf{V}(u)$ and $\mathbf{V} \mapsto J(\mathbf{V})$, using (9) and the equations (22) for the transverse field \mathbf{Z} . As is usual in PDE-constrained optimization, the gradient of the cost functional becomes apparent through the use of a so-called *adjoint state* \mathbf{R} . Since \mathbf{R} is adjoint to the transverse field \mathbf{Z} , we refer to it as the *adjoint transverse field*. Also, as \mathbf{Z} is a parabolic equation with initial conditions, \mathbf{R} is a backwards parabolic equation with terminal conditions. This is a well-known property for PDE-constrained optimization involving parabolic equations. We introduce the adjoint transverse field equations as

$$\begin{aligned} \partial_t \mathbf{R} + (D\mathbf{R})\mathbf{V} + A^*\mathbf{R} + \mu(t)\boldsymbol{\nu} &= -\phi\boldsymbol{\nu}, \quad \text{on } \Gamma^t(\mathbf{V}(u)) \text{ for all } t \in (0, t_f), \\ \int_{\Gamma^t(\mathbf{V}(u))} \mathbf{R}(t, \cdot) \cdot \boldsymbol{\nu}(t, \cdot) &= 0, \quad \text{for all } t \in (0, t_f), \\ \mathbf{R}(t_f, \cdot) &= 0, \quad \text{on } \Gamma^{t_f}(\mathbf{V}(u)), \end{aligned} \quad (24)$$

where μ is a Lagrange multiplier for the volume constraint in (24). The adjoint operator A^* is given by

$$A^*\mathbf{R} := \mathbf{R}\operatorname{div}_\Gamma(\mathbf{V}) + \operatorname{div}_\Gamma[(\mathbf{V} \cdot \boldsymbol{\nu})\mathbf{R}]\boldsymbol{\nu} + (D\mathbf{V})^\top \mathbf{R} + \Delta_\Gamma(\mathbf{R} \cdot \boldsymbol{\nu})\boldsymbol{\nu} - \kappa\mathbf{V}(\mathbf{R} \cdot \boldsymbol{\nu}) \quad \text{on } \Gamma^t(\mathbf{V}(u)). \quad (25)$$

Note that, since $D_{\mathbf{V}}\mathbf{R} \equiv \partial_t \mathbf{R} + (D\mathbf{R})\mathbf{V}$, we do not need \mathbf{R} extended, i.e. (24) is well-defined on the moving surface Γ^t . We obtain the following result.

Theorem 1. *The derivative of \mathcal{J} at u in the direction η is given by*

$$\mathcal{J}'(u; \eta) = \int_0^{t_f} \int_{\Gamma^t(\mathbf{V}(u))} \eta \mathbf{R} \cdot \boldsymbol{\nu} + \alpha \int_{\mathfrak{D}} \nabla u \cdot \nabla \eta, \quad (26)$$

where the adjoint transverse field \mathbf{R} is given by (24).

Proof. Using (9) and the chain rule, we get

$$\mathcal{J}'(u; \eta) = [\delta J(\mathbf{V}(u))](\mathbf{W}) = \int_0^{t_f} \int_{\Gamma^t(\mathbf{V}(u))} (\phi \boldsymbol{\nu}) \cdot \mathbf{Z} + \alpha \int_{\mathfrak{D}} \nabla u \cdot \nabla \eta.$$

Note that \mathbf{Z} solution of (22) is (indirectly) a function of η . Using (24) we get

$$\mathcal{J}'(u; \eta) = \int_0^{t_f} \int_{\Gamma^t(\mathbf{V}(u))} \underbrace{-[\partial_t \mathbf{R} + (D\mathbf{R})\mathbf{V} + A^* \mathbf{R} + \mu(t)\boldsymbol{\nu}]}_{\equiv D_{\mathbf{V}} \mathbf{R}} \cdot \mathbf{Z} + \alpha \int_{\mathfrak{D}} \nabla u \cdot \nabla \eta.$$

Let us define

$$\begin{aligned} L_1 &:= \int_0^{t_f} \int_{\Gamma^t(\mathbf{V}(u))} -(D_{\mathbf{V}} \mathbf{R}) \cdot \mathbf{Z} \\ &= - \int_0^{t_f} \frac{d}{dt} \int_{\Gamma^t(\mathbf{V}(u))} \mathbf{R} \cdot \mathbf{Z} + \int_0^{t_f} \int_{\Gamma^t(\mathbf{V}(u))} \mathbf{R} \cdot D_{\mathbf{V}} \mathbf{Z} + (\mathbf{R} \cdot \mathbf{Z}) \operatorname{div}_{\Gamma}(\mathbf{V}), \\ L_2 &:= \int_0^{t_f} \int_{\Gamma^t(\mathbf{V}(u))} -(A^* \mathbf{R} + \mu(t)\boldsymbol{\nu}) \cdot \mathbf{Z} = \int_0^{t_f} \int_{\Gamma^t(\mathbf{V}(u))} -(A^* \mathbf{R}) \cdot \mathbf{Z}, \end{aligned}$$

where we used (22) and standard relations for shape derivatives [35]. Proceeding with L_1 , and noting that boundary terms drop because of the terminal and initial conditions in (24) and (22), we get

$$\begin{aligned} L_1 &= \int_0^{t_f} \int_{\Gamma^t(\mathbf{V}(u))} \mathbf{R} \cdot D_{\mathbf{V}} \mathbf{Z} + (\mathbf{R} \cdot \mathbf{Z}) \operatorname{div}_{\Gamma}(\mathbf{V}) \\ &= \int_0^{t_f} \int_{\Gamma^t(\mathbf{V}(u))} -\mathbf{R} \cdot (-\mathbf{Z} \operatorname{div}_{\Gamma}(\mathbf{V}) + A\mathbf{Z} + \rho \boldsymbol{\nu} - \eta \boldsymbol{\nu}) \\ &= \int_0^{t_f} \int_{\Gamma^t(\mathbf{V}(u))} -\mathbf{R} \cdot \{-\mathbf{Z} \operatorname{div}_{\Gamma}(\mathbf{V}) - (D\mathbf{V})\mathbf{Z} - \Delta_{\Gamma}(\mathbf{Z} \cdot \boldsymbol{\nu})\boldsymbol{\nu} + (u - \kappa - \lambda) \nabla_{\Gamma}(\mathbf{Z} \cdot \boldsymbol{\nu}) - \eta \boldsymbol{\nu}\}, \end{aligned}$$

where we used the mean value zero condition in (24).

Note from Lemma 1 (using the fact that $\Gamma^t(\mathbf{V}(u))$ is a manifold without boundary) that

$$\int_0^{t_f} \int_{\Gamma^t(\mathbf{V}(u))} \Delta_{\Gamma}(\mathbf{Z} \cdot \boldsymbol{\nu}) \mathbf{R} \cdot \boldsymbol{\nu} = \int_0^{t_f} \int_{\Gamma^t(\mathbf{V}(u))} \Delta_{\Gamma}(\mathbf{R} \cdot \boldsymbol{\nu}) \mathbf{Z} \cdot \boldsymbol{\nu},$$

and integration by parts gives

$$\begin{aligned} &\int_0^{t_f} \int_{\Gamma^t(\mathbf{V}(u))} -(u - \kappa - \lambda) \mathbf{R} \cdot \nabla_{\Gamma}(\mathbf{Z} \cdot \boldsymbol{\nu}) \\ &= \int_0^{t_f} \int_{\Gamma^t(\mathbf{V}(u))} (\mathbf{Z} \cdot \boldsymbol{\nu}) \operatorname{div}_{\Gamma}[(u - \kappa - \lambda) \mathbf{R}] - \kappa (\mathbf{Z} \cdot \boldsymbol{\nu}) (u - \kappa - \lambda) \mathbf{R} \cdot \boldsymbol{\nu} \\ &= \int_0^{t_f} \int_{\Gamma^t(\mathbf{V}(u))} \mathbf{Z} \cdot [\operatorname{div}_{\Gamma}[(\mathbf{V} \cdot \boldsymbol{\nu}) \mathbf{R}] \boldsymbol{\nu} - \kappa \mathbf{V}(\mathbf{R} \cdot \boldsymbol{\nu})], \end{aligned}$$

where we used $\mathbf{V} = (u - \kappa - \lambda)\boldsymbol{\nu}$ on $\Gamma^t(\mathbf{V}(u))$. Gathering these results, and using (25), we obtain (26). \square

3.4 Normal transverse field and scalar adjoint

In Section 3.2 we have derived the system of equations (22) for the transverse field \mathbf{Z} associated with the perturbation of $\mathcal{J}(u)$. Since the derivative (9) only depends on the normal component $\mathbf{Z} \cdot \boldsymbol{\nu}$ of \mathbf{Z} , it is natural to ask whether $\mathbf{Z} \cdot \boldsymbol{\nu}$ and the tangential component of \mathbf{Z} may be fully decoupled. Indeed, for numerical applications it is more convenient to solve only for $\mathbf{Z} \cdot \boldsymbol{\nu}$ instead of \mathbf{Z} . In this section we show that the normal component can indeed be decoupled and that $\mathbf{Z} \cdot \boldsymbol{\nu}$ satisfies an evolution equation similar to (22).

We introduce the simpler notation $Z_\nu := \mathbf{Z} \cdot \boldsymbol{\nu}$. Referring to (22), (23), we derive a stand-alone equation for Z_ν . Projecting the first equation in (22) onto $\boldsymbol{\nu}$, we get

$$\begin{aligned} \eta &= (D_{\mathbf{V}}\mathbf{Z}) \cdot \boldsymbol{\nu} - \boldsymbol{\nu}^\top (D\mathbf{V})\mathbf{Z} - \Delta_\Gamma(\mathbf{Z} \cdot \boldsymbol{\nu}) + \rho \\ &= D_{\mathbf{V}}(\mathbf{Z} \cdot \boldsymbol{\nu}) - \mathbf{Z} \cdot (D_{\mathbf{V}}\boldsymbol{\nu}) - \boldsymbol{\nu}^\top (D\mathbf{V})\mathbf{Z} - \Delta_\Gamma Z_\nu + \rho \\ &= D_{\mathbf{V}}(\mathbf{Z} \cdot \boldsymbol{\nu}) + \boldsymbol{\nu}^\top (D_\Gamma \mathbf{V})\mathbf{Z} - \boldsymbol{\nu}^\top (D\mathbf{V})\mathbf{Z} - \Delta_\Gamma Z_\nu + \rho \\ &= D_{\mathbf{V}}Z_\nu - (\boldsymbol{\nu}^\top (D\mathbf{V})\boldsymbol{\nu})Z_\nu - \Delta_\Gamma Z_\nu + \rho, \end{aligned} \tag{27}$$

where we used that $D_{\mathbf{V}}\boldsymbol{\nu} = -(D_\Gamma \mathbf{V})^\top \boldsymbol{\nu}$ (see [35, Eqn. (5.38)]). Noting that

$$\partial_\nu(u - \kappa) = \partial_\nu(\mathbf{V} \cdot \boldsymbol{\nu}) = \boldsymbol{\nu}^\top (D\mathbf{V})\boldsymbol{\nu} + \underbrace{\mathbf{V}^\top (D\boldsymbol{\nu})\boldsymbol{\nu}}_{=0}, \tag{28}$$

we obtain the following stand-alone evolution equation for Z_ν :

$$\begin{aligned} D_{\mathbf{V}}Z_\nu - \partial_\nu(u - \kappa)Z_\nu - \Delta_\Gamma Z_\nu + \rho &= \eta, \quad \text{on } \Gamma^t(\mathbf{V}(u)) \text{ for all } t \in (0, t_f), \\ \int_{\Gamma^t(\mathbf{V}(u))} Z_\nu(t, \cdot) &= 0, \quad \text{for all } t \in (0, t_f), \\ Z_\nu(0, \cdot) &= 0, \quad \text{on } \Gamma^0(\mathbf{V}(u)). \end{aligned} \tag{29}$$

In Section 3.3 we have introduced the adjoint transverse field \mathbf{R} to compute the derivative (26). Since we have obtained a stand-alone system of equations (29) for the normal transverse field Z_ν and since the derivative (9) only depends on Z_ν , we just need a scalar adjoint to compute the derivative $\mathcal{J}'(u; \eta)$. Therefore we introduce a scalar adjoint state R satisfying the following backwards evolution equation with terminal conditions:

$$\begin{aligned} D_{\mathbf{V}}R + A_\Gamma^* R + \mu(t) &= -\phi, \quad \text{on } \Gamma^t(\mathbf{V}(u)) \text{ for all } t \in (0, t_f), \\ \int_{\Gamma^t(\mathbf{V}(u))} R(t, \cdot) &= 0, \quad \text{for all } t \in (0, t_f), \\ R(t_f, \cdot) &= 0, \quad \text{on } \Gamma^{t_f}(\mathbf{V}(u)), \end{aligned} \tag{30}$$

where μ is a Lagrange multiplier for the volume constraint in (30) and

$$\begin{aligned} A_\Gamma^* R &:= R \operatorname{div}_\Gamma(\mathbf{V}) + R \partial_\nu(u - \kappa) + \Delta_\Gamma R \\ &= R \operatorname{div}_\Gamma(\mathbf{V}) + R \boldsymbol{\nu}^\top (D\mathbf{V})\boldsymbol{\nu} + \Delta_\Gamma R \\ &= R \operatorname{div}[(\mathbf{V} \cdot \boldsymbol{\nu})\boldsymbol{\nu}] + \Delta_\Gamma R = R \partial_\nu(u - \kappa) + R(\mathbf{V} \cdot \boldsymbol{\nu})\kappa + \Delta_\Gamma R. \end{aligned} \tag{31}$$

The well-posedness for the equations of Z_ν and R may be proven using the abstract framework for parabolic PDEs on evolving spaces developed in [1, 2].

We can now compute $\mathcal{J}'(u; \eta)$ using the scalar adjoint transverse field R ; this provides an alternative to Theorem 1 for computing $\mathcal{J}'(u; \eta)$.

Theorem 2. *The derivative of \mathcal{J} at u in the direction η is given by*

$$\mathcal{J}'(u; \eta) = \int_0^{t_f} \int_{\Gamma^t(\mathbf{V}(u))} R\eta + \alpha \int_{\mathfrak{D}} \nabla u \cdot \nabla \eta, \quad (32)$$

where the scalar adjoint state R is given by (30).

Proof. Using (9) and the chain rule, we get

$$\mathcal{J}'(u; \eta) = [\delta J(\mathbf{V}(u))](\mathbf{W}) = \int_0^{t_f} \int_{\Gamma^t(\mathbf{V}(u))} \phi Z_\nu + \alpha \int_{\mathfrak{D}} \nabla u \cdot \nabla \eta.$$

Note that Z_ν solution of (29) is a function of η . Using (30), we get

$$\mathcal{J}'(u; \eta) = \int_0^{t_f} \int_{\Gamma^t(\mathbf{V}(u))} -Z_\nu [D_{\mathbf{V}}R + A_\Gamma^* R + \mu(t)] + \alpha \int_{\mathfrak{D}} \nabla u \cdot \nabla \eta.$$

Noting that

$$\int_0^{t_f} \int_{\Gamma^t(\mathbf{V}(u))} -Z_\nu D_{\mathbf{V}}R = - \int_0^{t_f} \frac{d}{dt} \int_{\Gamma^t(\mathbf{V}(u))} Z_\nu R + \int_0^{t_f} \int_{\Gamma^t(\mathbf{V}(u))} R D_{\mathbf{V}}Z_\nu + R Z_\nu \operatorname{div}_{\Gamma}(\mathbf{V}),$$

using the initial and terminal conditions, and (29), gives

$$\begin{aligned} \int_0^{t_f} \int_{\Gamma^t(\mathbf{V}(u))} -Z_\nu D_{\mathbf{V}}R &= \int_0^{t_f} \int_{\Gamma^t(\mathbf{V}(u))} R [\partial_\nu(u - \kappa)Z_\nu + \Delta_\Gamma Z_\nu - \rho(t) + \eta] + R Z_\nu \operatorname{div}_{\Gamma}(\mathbf{V}) \\ &= \int_0^{t_f} \int_{\Gamma^t(\mathbf{V}(u))} Z_\nu [R \operatorname{div}_{\Gamma}(\mathbf{V}) + R \partial_\nu(u - \kappa) + \Delta_\Gamma R] + R\eta \\ &= \int_0^{t_f} \int_{\Gamma^t(\mathbf{V}(u))} Z_\nu A_\Gamma^* R + R\eta, \end{aligned}$$

where we used the mean value zero property, and integrated by parts. The result then follows. \square

It is worthwhile to check if the perturbation field \mathbf{W} solution of (20) is such that $\mathbf{W} \cdot \boldsymbol{\nu}$ is mean value zero on Γ^t . Recalling (20), (22), and applying a similar argument as in (27), we have

$$D_{\mathbf{V}}Z_\nu - (\boldsymbol{\nu}^\top(D\mathbf{V})\boldsymbol{\nu})Z_\nu = \mathbf{W} \cdot \boldsymbol{\nu}, \text{ on } \Gamma^t(\mathbf{V}(u)) \text{ for all } t \in (0, t_f). \quad (33)$$

Integrating over Γ^t , we then get

$$\int_{\Gamma^t} D_{\mathbf{V}}Z_\nu + Z_\nu \operatorname{div}_{\Gamma}(\mathbf{V}) - \int_{\Gamma^t} Z_\nu [\operatorname{div}_{\Gamma}(\mathbf{V}) + (\boldsymbol{\nu}^\top(D\mathbf{V})\boldsymbol{\nu})] = \int_{\Gamma^t} \mathbf{W} \cdot \boldsymbol{\nu}, \quad (34)$$

or actually

$$\frac{d}{dt} \int_{\Gamma^t} Z_\nu - \int_{\Gamma^t} Z_\nu \operatorname{div} \mathbf{V} = \int_{\Gamma^t} \mathbf{W} \cdot \boldsymbol{\nu}, \quad (35)$$

for all $t \in (0, t_f)$. Since Z_ν is mean value zero for all $t \in (0, t_f)$, then $\mathbf{W} \cdot \boldsymbol{\nu}$ is also mean value zero, *provided* \mathbf{V} is extended in a divergence free way. This is certainly possible to do since $\mathbf{V} \cdot \boldsymbol{\nu}$ is mean value zero. However, it is not necessary that this be done; we do not explicitly use \mathbf{W} . In other words, for the numerical scheme we use, it is not necessary that \mathbf{W} be mean value zero.

3.5 Decoupling the normal and tangential components of the adjoint

Comparing the two expressions (26) and (32) of the derivative $\mathcal{J}'(u; \eta)$ indicates that $R \equiv \mathbf{R} \cdot \boldsymbol{\nu}$ on $\Gamma^t(\mathbf{V}(u))$. We show that the normal component $\mathbf{R} \cdot \boldsymbol{\nu}$ and the tangential component \mathbf{R}_Γ of \mathbf{R} can indeed be explicitly decoupled, but interestingly the proof is much less straightforward than the similar decoupling for \mathbf{Z} that we have performed in Section 3.4. In fact we have to show that the tangential component \mathbf{R}_Γ vanishes.

Define the time-dependent tangent space projection $\mathbf{P} = \mathbf{I} - \boldsymbol{\nu} \otimes \boldsymbol{\nu}$ on Γ^t , and set $\mathbf{R}_\Gamma := \mathbf{P}\mathbf{R}$ where \mathbf{R} solves (24). Next, we derive an evolution equation for \mathbf{R}_Γ . Preliminary calculations give

$$\begin{aligned} \mathbf{P}D_{\mathbf{V}}\mathbf{R} &= D_{\mathbf{V}}\mathbf{R}_\Gamma + [D_{\mathbf{V}}(\boldsymbol{\nu} \otimes \boldsymbol{\nu})]\mathbf{R} = D_{\mathbf{V}}\mathbf{R}_\Gamma + D_{\mathbf{V}}\boldsymbol{\nu}(\mathbf{R} \cdot \boldsymbol{\nu}) + \boldsymbol{\nu}[(D_{\mathbf{V}}\boldsymbol{\nu}) \cdot \mathbf{R}], \\ &= D_{\mathbf{V}}\mathbf{R}_\Gamma - (D_\Gamma\mathbf{V})^\top \boldsymbol{\nu}(\mathbf{R} \cdot \boldsymbol{\nu}) - \boldsymbol{\nu}[\boldsymbol{\nu}^\top (D_\Gamma\mathbf{V})\mathbf{R}_\Gamma], \end{aligned} \quad (36)$$

where we used $D_{\mathbf{V}}\boldsymbol{\nu} = -(D_\Gamma\mathbf{V})^\top \boldsymbol{\nu}$ (see [35, Eqn. (5.38)]), and

$$\mathbf{P}(A^*\mathbf{R}) = \mathbf{R}_\Gamma \operatorname{div}_\Gamma(\mathbf{V}) + (D_\Gamma\mathbf{V})^\top \mathbf{R} - \kappa(\mathbf{R} \cdot \boldsymbol{\nu})\mathbf{P}\mathbf{V}, \quad (37)$$

noting that $\mathbf{P}\mathbf{V} = \mathbf{0}$ and using (31). Using the above, applying \mathbf{P} to (24) yields

$$\begin{aligned} D_{\mathbf{V}}\mathbf{R}_\Gamma + (D_\Gamma\mathbf{V})^\top \mathbf{P}\mathbf{R} - [\boldsymbol{\nu}^\top (D_\Gamma\mathbf{V})\mathbf{R}_\Gamma]\boldsymbol{\nu} + \mathbf{R}_\Gamma \operatorname{div}_\Gamma(\mathbf{V}) &= \mathbf{0}, \quad \text{on } \Gamma^t(\mathbf{V}(u)) \text{ for all } t \in (0, t_f), \\ \mathbf{R}_\Gamma(t_f, \cdot) &= \mathbf{0}, \quad \text{on } \Gamma^{t_f}(\mathbf{V}(u)), \end{aligned} \quad (38)$$

or equivalently

$$\begin{aligned} D_{\mathbf{V}}\mathbf{R}_\Gamma + \left[(D_\Gamma\mathbf{V})^\top - (\boldsymbol{\nu} \otimes \boldsymbol{\nu})(D_\Gamma\mathbf{V}) + \mathbf{I} \operatorname{div}_\Gamma(\mathbf{V}) \right] \mathbf{R}_\Gamma &= \mathbf{0}, \quad \text{on } \Gamma^t(\mathbf{V}(u)) \text{ for all } t \in (0, t_f), \\ \mathbf{R}_\Gamma(t_f, \cdot) &= \mathbf{0}, \quad \text{on } \Gamma^{t_f}(\mathbf{V}(u)), \end{aligned} \quad (39)$$

which can be viewed as a simple ODE for \mathbf{R}_Γ with zero right-hand-side and vanishing initial condition. Thus, $\mathbf{R}_\Gamma \equiv \mathbf{0}$ for all $\mathbf{x} \in \Gamma^t$ and all $t \in (0, t_f)$.

Thus, $\mathbf{R} = r\boldsymbol{\nu}$, for some scalar valued function r , so then (24) reduces to

$$\begin{aligned} D_{\mathbf{V}}(r\boldsymbol{\nu}) + A^*(r\boldsymbol{\nu}) + \mu(t)\boldsymbol{\nu} &= -\phi\boldsymbol{\nu}, \quad \text{on } \Gamma^t(\mathbf{V}(u)) \text{ for all } t \in (0, t_f), \\ \int_{\Gamma^t(\mathbf{V}(u))} r(t, \cdot) &= 0, \quad \text{for all } t \in (0, t_f), \\ r(t_f, \cdot) &= 0, \quad \text{on } \Gamma^{t_f}(\mathbf{V}(u)). \end{aligned} \quad (40)$$

Upon noting that $\operatorname{div}_\Gamma[(\mathbf{V} \cdot \boldsymbol{\nu})r\boldsymbol{\nu}] = (\mathbf{V} \cdot \boldsymbol{\nu})r \operatorname{div}_\Gamma(\boldsymbol{\nu}) = (\mathbf{V} \cdot \boldsymbol{\nu})r\kappa$, the first line of (40) becomes

$$\begin{aligned} -\phi\boldsymbol{\nu} &= \boldsymbol{\nu}D_{\mathbf{V}}r + rD_{\mathbf{V}}\boldsymbol{\nu} + r\boldsymbol{\nu} \operatorname{div}_\Gamma(\mathbf{V}) + (\mathbf{V} \cdot \boldsymbol{\nu})r\kappa\boldsymbol{\nu} + r(D\mathbf{V})^\top \boldsymbol{\nu} + \boldsymbol{\nu}\Delta_\Gamma r - \kappa\mathbf{V}r + \mu(t)\boldsymbol{\nu}, \\ &= \boldsymbol{\nu}D_{\mathbf{V}}r - r(D_\Gamma\mathbf{V})^\top \boldsymbol{\nu} + r\boldsymbol{\nu} \operatorname{div}_\Gamma(\mathbf{V}) + (\mathbf{V} \cdot \boldsymbol{\nu})r\kappa\boldsymbol{\nu} + r(D\mathbf{V})^\top \boldsymbol{\nu} + \boldsymbol{\nu}\Delta_\Gamma r - \kappa\mathbf{V}r + \mu(t)\boldsymbol{\nu}, \end{aligned} \quad (41)$$

on $\Gamma^t(\mathbf{V}(u))$ for all $t \in (0, t_f)$. Taking the dot product with $\boldsymbol{\nu}$, and using (28), we arrive at

$$\begin{aligned} -\phi &= D_{\mathbf{V}}r + r \operatorname{div}_\Gamma(\mathbf{V}) + (\mathbf{V} \cdot \boldsymbol{\nu})r\kappa + r\boldsymbol{\nu}^\top (D\mathbf{V})\boldsymbol{\nu} + \Delta_\Gamma r - \kappa(\mathbf{V} \cdot \boldsymbol{\nu})r + \mu(t) \\ &= D_{\mathbf{V}}r + r \operatorname{div}_\Gamma(\mathbf{V}) + r\partial_{\boldsymbol{\nu}}(u - \kappa) + \Delta_\Gamma r + \mu(t), \end{aligned} \quad (42)$$

on $\Gamma^t(\mathbf{V}(u))$ for all $t \in (0, t_f)$. Therefore, r solves the scalar adjoint equation in (30). Since the solution is unique we obtain $r \equiv R$ and consequently $R \equiv \mathbf{R} \cdot \boldsymbol{\nu}$.

4 Optimization method

We present the basic method for computing a local minimizer of (7). This discussion is formal in the sense that we assume no topological changes in the forward problem, that the objective functionals are sufficiently smooth, etc. Algorithm 1 gives the optimization scheme for the continuous problem. In the subsequent sections, we take the optimize then discretize approach, i.e. we follow Algorithm 1 and simply replace each step by the fully discrete finite element version.

Algorithm 1 Continuous gradient flow algorithm.

Define ϕ , $\alpha > 0$, $t_f > 0$, $\text{TOL} > 0$, and initialize Ω_0^0 or (equivalently) Γ_0^0 . Set an initial guess for the control u_0 , e.g. $u_0 := 0$. For $k \geq 0$, do the following.

1. Forward problem. Solve (3) on the interval $(0, t_f]$ using u_k , i.e. compute Γ_k^t for all $t \in (0, t_f]$.
2. Adjoint problem. Solve (30) on Γ_k^t to obtain $R_k(t)$ for all $t \in [0, t_f]$.
3. Descent Direction. Solve the following variational problem: find $\eta_{k+1} \in H_0^1(\mathfrak{D})$ such that

$$a(\eta_{k+1}, \xi) = -\mathcal{J}'(u_k; \xi) = -\int_0^{t_f} \int_{\Gamma_k^t} R_k \xi - \alpha \int_{\mathfrak{D}} \nabla u_k \cdot \nabla \xi, \quad \forall \xi \in H_0^1(\mathfrak{D}), \quad (43)$$

where $a(\cdot, \cdot)$ is some useful symmetric bilinear form (inner product).

4. Backtracking line-search:

- (a) Initialize the step-size $\rho_{k+1} := 1$.
- (b) Trial update. $u_{k+1} := u_k + \rho_{k+1} \eta_{k+1}$.
- (c) Check for cost decrease. If

$$\mathcal{J}(u_{k+1}) < \mathcal{J}(u_k) \quad (44)$$

then we accept u_{k+1} and go to step 5. Otherwise, replace $\rho_{k+1} \leftarrow \rho_{k+1}/2$, and go back to step 4(b), and repeat.

5. Terminate. If $|\mathcal{J}(u_{k+1}) - \mathcal{J}(u_k)| < \text{TOL}$, then stop. Otherwise, $k \leftarrow k + 1$, and go to step 1.
-

4.1 Discretization

For simplicity, we will have a uniform time discretization, but this is not necessary. Thus, we have a set of discrete time points $\{t_i\}_{i=0}^N$, where $t_0 = 0$, $t_N = t_f$, and $t_{i+1} - t_i = \delta t$ (for all i). Moreover, the surface evolution will be captured by a finite set of surfaces $\{\Gamma^i\}_{i=0}^N$, the evolution of which is specified in Section 4.2. Each Γ^i is a triangulated surface with curved triangles. For simplicity of notation, we do not use a subscript h for Γ , u , η , and R . In other words, all solution variables here are discrete, finite element functions.

4.1.1 Standard finite element spaces

Let \mathcal{T}_h be a conforming, shape regular triangulation of \mathfrak{D} (that is not fitted to Γ^i , for all i), and let \mathcal{G}_h^i be a conforming, shape regular curved *surface* triangulation of Γ^i .

Let \mathbb{S}_h^q be the space of continuous Lagrange finite elements over \mathcal{T}_h of degree $q \geq 1$, with standard

interpolation operator I_h^q ; moreover, let \mathbb{S}_h^0 be the space of piecewise constants on \mathcal{T}_h with projection operator I_h^0 . In addition, let $S_h^q(\Gamma^i)$ be the space of continuous Lagrange finite elements over \mathcal{G}_h^i of degree $q \geq 1$, with standard interpolation operator $\pi_h^{i,q}$; moreover, let $S_h^0(\Gamma^i)$ be the space of piecewise constants on \mathcal{G}_h^i with projection operator $\pi_h^{i,0}$. We usually simplify notation and drop the polynomial degree. We also have the L^2 projection operator: $P_h^q : L^2(\mathcal{D}) \rightarrow \mathbb{S}_h^q$, for any $q \geq 0$.

Next, we have the following discrete, bulk finite element spaces:

$$\mathbb{U}_h(g) := \mathbb{S}_h^q \cap [g + H_0^1(\mathcal{D})], \quad (45)$$

and the following discrete surface finite element spaces:

$$Y_h(\Gamma^i) := S_h^q(\Gamma^i), \quad (46)$$

where $q \geq 1$. In dealing with the evolving surfaces, we require the ‘‘obvious’’ transfer operator: $\Pi_{i-1}^i : Y_h(\Gamma^{i-1}) \rightarrow Y_h(\Gamma^i)$, i.e. if $\mathbf{x} \in [Y_h(\Gamma^{i-1})]^n$, then $\tilde{\mathbf{x}} := \pi_h^i[\mathbf{x} \circ \Phi^{-1}] \in [Y_h(\Gamma^i)]^n$, where $\Phi : \Gamma^{i-1} \rightarrow \Gamma^i$.

4.1.2 Geometric quantities

We have access to the additive curvature κ , as well as the normal velocity through our method for the forward problem (Section 4.2). We also need the so-called *shape operator* $D_\Gamma \boldsymbol{\nu}$ due to the following identity (48). Suppose $\boldsymbol{\nu}$ is extended constant in the normal direction, then $\partial_\nu \boldsymbol{\nu} = (D\boldsymbol{\nu})\boldsymbol{\nu} = \mathbf{0}$ and $\kappa = \text{div } \boldsymbol{\nu}$; see [35]. Furthermore,

$$\begin{aligned} 0 &= \text{div} [(D\boldsymbol{\nu})\boldsymbol{\nu}] = \partial_i [(\partial_j \nu_i) \nu_j] = (\partial_j \partial_i \nu_i) \nu_j + (\partial_j \nu_i) (\partial_i \nu_j) \\ &= \partial_\nu (\text{div } \boldsymbol{\nu}) + (D\boldsymbol{\nu})^\top : (D\boldsymbol{\nu}) = \partial_\nu \kappa + (D\boldsymbol{\nu}) : (D\boldsymbol{\nu}) \\ &= \partial_\nu \kappa + |D_\Gamma \boldsymbol{\nu}|^2, \end{aligned} \quad (47)$$

where we used that $D\boldsymbol{\nu} = D_\Gamma \boldsymbol{\nu}$ (the shape operator) is a symmetric matrix. Therefore,

$$\partial_\nu \kappa = -|D_\Gamma \boldsymbol{\nu}|^2. \quad (48)$$

In other words, we do not need an extension to compute $\partial_\nu \kappa$. Note that $|D_\Gamma \boldsymbol{\nu}|^2$ is also equal to the sum of squares of the principal curvatures; see [11, p. 317].

4.2 Discretization of the forward problem

We use a variation of the Barrett-Garcke-Nürnberg method [9, 8]. The sequence of $\{\Gamma^i\}$ will be represented by the following set of finite element functions: $\{\mathbf{x}^i\}_{i=0}^N$, where $\mathbf{x}^0 \equiv \text{id}_{\Gamma^0} \in [Y_h(\Gamma^0)]^n$, $\mathbf{X}^{i+1} \in [Y_h(\Gamma^i)]^n$, for $0 \leq i \leq N-1$, and $\Gamma^{i+1} := \pi_h^i[\mathbf{X}^{i+1}(\Gamma^i)]$, for $0 \leq i \leq N-1$.

More specifically, given $u \in \mathbb{U}_h(0)$, Γ^i , we find $\mathbf{X}^{i+1} \in [Y_h(\Gamma^i)]^n$, $\hat{\kappa}^{i+1} \in Y_h(\Gamma^i)$, $\lambda^{i+1} \in \mathbb{R}$ such that

$$\begin{aligned} (D_\Gamma \mathbf{X}^{i+1}, D_\Gamma \mathbf{Y})_{\Gamma^i} - (\hat{\kappa}^{i+1}, \mathbf{Y} \cdot \boldsymbol{\nu})_{\Gamma^i} + \lambda^{i+1} (1, \mathbf{Y} \cdot \boldsymbol{\nu})_{\Gamma^i} &= 0, \quad \forall \mathbf{Y} \in [Y_h(\Gamma^i)]^n, \\ -(\mathbf{X}^{i+1} \cdot \boldsymbol{\nu}, v)_{\Gamma^i} - \delta t (\hat{\kappa}^{i+1}, v)_{\Gamma^i} &= -(\text{id}_{\Gamma^i} \cdot \boldsymbol{\nu}, v)_{\Gamma^i} - \delta t (\pi_h^i u, v)_{\Gamma^i}, \quad \forall v \in Y_h(\Gamma^i), \\ (\mathbf{X}^{i+1} \cdot \boldsymbol{\nu}, 1)_{\Gamma^i} &= (\text{id}_{\Gamma^i} \cdot \boldsymbol{\nu}, 1)_{\Gamma^i}, \\ \kappa^{i+1} &:= \hat{\kappa}^{i+1} - \lambda^{i+1} \in Y_h(\Gamma^i), \\ \mathbf{V}^{i+1} &:= \pi_h^i \left[\frac{\mathbf{X}^{i+1} - \text{id}_{\Gamma^i}}{\delta t} \right] \in [Y_h(\Gamma^i)]^n, \end{aligned} \quad (49)$$

where κ^{i+1} is an approximation of the additive curvature of Γ^i . The main distinction here between this method and the various methods of Barrett-Garcke-Nürnberg [9, 8], is that we *do not* use mass-lumped inner products. The reason for this is we compute the shape operator in (48) explicitly using the curved surface mesh (this is for solving the adjoint problem). The methods in [9, 8] are entirely formulated on piecewise linear surface triangulations.

Let us now relate the formulation (49) to the continuous problem. Taking the mesh size to zero, and integrating the first equation in (49) by parts, we see that

$$-(\Delta_\Gamma \mathbf{X}^{i+1}, \mathbf{Y})_{\Gamma^i} = (\hat{\kappa}^{i+1} - \lambda^{i+1}, \mathbf{Y} \cdot \boldsymbol{\nu})_{\Gamma^i}, \quad \forall \mathbf{Y} \in [Y_h(\Gamma^i)]^n. \quad (50)$$

Next, formally taking $\delta t \rightarrow 0$, this becomes

$$(\kappa, \mathbf{Y} \cdot \boldsymbol{\nu})_{\Gamma^t} = (-\Delta_{\Gamma^t} \text{id}_{\Gamma^t}, \mathbf{Y})_{\Gamma^t} = (\hat{\kappa} - \lambda, \mathbf{Y} \cdot \boldsymbol{\nu})_{\Gamma^t}, \quad \forall \mathbf{Y} \in [H^1(\Gamma^t)]^n, \quad (51)$$

where we used the identity $-\Delta_{\Gamma^t} \text{id}_{\Gamma^t} \equiv \kappa \boldsymbol{\nu}$. Thus, $\kappa = \hat{\kappa} - \lambda$. In addition, taking the mesh size to zero and $\delta t \rightarrow 0$, the third equation in (49) yields

$$(\mathbf{V} \cdot \boldsymbol{\nu}, 1)_{\Gamma^t} = 0, \quad \forall t \in [0, t_f]. \quad (52)$$

Lastly, the second equation in (49) becomes

$$(\mathbf{V} \cdot \boldsymbol{\nu}, v)_{\Gamma^t} = (u - \hat{\kappa}, v)_{\Gamma^t} = (u - \kappa - \lambda, v)_{\Gamma^t}, \quad \forall v \in H^1(\Gamma^t), \quad (53)$$

which matches (3).

4.3 Discretization of the adjoint

Now that we have the sequence $\{\Gamma^i\}$, solving the adjoint problem (numerically) is relatively straightforward. Note that the adjoint evolution problem is solved *backward* in time; see (30). We begin by discretizing the material derivative $D_{\mathbf{V}}R$:

$$(D_{\mathbf{V}}R)(t_i, \cdot) \approx \frac{R^i - \tilde{R}^{i+1}}{-\delta t}, \quad \text{on } \Gamma^i, \quad \text{with } \tilde{R}^i = \pi_h^{i-1} \Pi_i^{i-1} R^i, \quad (54)$$

where $\tilde{R}^i \in Y_h(\Gamma^{i-1})$, $R^{i-1} \in Y_h(\Gamma^{i-1})$, for all $1 \leq i \leq N$. Next, let $\mathbf{g} := \pi_h^i P_h(Du) \in \mathbb{U}_h$ (L^2 projection). Then, given $\tilde{R}^N := 0$, we do the following for $i = N-1, \dots, 2, 1, 0$. Find $R^i \in Y_h(\Gamma^i)$ and $\mu^i \in \mathbb{R}$ such that

$$\begin{aligned} & \left(\frac{R^i - \tilde{R}^{i+1}}{-\delta t}, Y \right)_{\Gamma^i} + (R^i \text{div}_{\Gamma^i}(\mathbf{V}^{i+1}), Y)_{\Gamma^i} - (D_\Gamma R^i, D_\Gamma Y)_{\Gamma^i} \\ & + (R^i \boldsymbol{\nu}^i \cdot \mathbf{g}, Y)_{\Gamma^i} + (R^i |D_{\Gamma^i} \boldsymbol{\nu}^i|^2, Y)_{\Gamma^i} + \mu^i (1, Y)_{\Gamma^i} = -(\pi_h^i \phi(t_i, \cdot), Y)_{\Gamma^i}, \quad \forall Y \in Y_h(\Gamma^i), \\ & (R^i, 1)_{\Gamma^i} = 0. \end{aligned} \quad (55)$$

Note that the Laplace term seems to have the “wrong sign”, but the time-step is negative.

4.4 Discrete optimization method

The discrete optimization algorithm method mirrors Algorithm 1. The discrete cost is defined by

$$\mathcal{J}_h(u) := \sum_{i=0}^N \omega_i \int_{\Omega^i(u)} \phi(t_i, \cdot) + \frac{\alpha}{2} \|\nabla u\|_{L^2(\mathcal{D})}^2, \quad \forall u \in \mathbb{U}_h(0), \quad (56)$$

where ω_i are quadrature weights for the time integral (e.g. one can use the trapezoidal rule). Algorithm 2 gives the fully discrete method.

Algorithm 2 Discrete gradient flow algorithm.

Define ϕ , $\alpha > 0$, $t_f > 0$, $N = t_f/\delta t$, $\text{TOL} > 0$, and initialize Ω_0^0 or (equivalently) Γ_0^0 . Set an initial guess for the control u_0 , e.g. $u_0 := 0$. For $k \geq 0$, do the following.

1. Forward problem. Solve (49) using u_k , i.e. compute $\{\Gamma_k^i\}_{i=0}^N$.
2. Adjoint problem. Solve (55) on $\{\Gamma_k^i\}_{i=0}^N$ to obtain $\{R_k^i\}_{i=0}^N$.
3. Descent Direction. Solve the following variational problem: find $\eta_{k+1} \in \mathbb{U}_h(0)$ such that

$$a(\eta_{k+1}, \xi) = - \sum_{i=0}^N \omega_i \int_{\Gamma_k^i} R_k^i(\pi_h^i \xi) - \alpha \int_{\mathcal{D}} \nabla u_k \cdot \nabla \xi, \quad \forall \xi \in \mathbb{U}_h(0). \quad (57)$$

4. Backtracking line-search:

- (a) Initialize the step-size $\rho_{k+1} := 1$.
- (b) Trial update. $u_{k+1} := u_k + \rho_{k+1} \eta_{k+1}$.
- (c) Check for cost decrease. If

$$\mathcal{J}_h(u_{k+1}) < \mathcal{J}_h(u_k) \quad (58)$$

then we accept u_{k+1} and go to step 5. Otherwise, replace $\rho_{k+1} \leftarrow \rho_{k+1}/2$, and go back to step 4(b), and repeat.

5. Terminate. If $|\mathcal{J}_h(u_{k+1}) - \mathcal{J}_h(u_k)| < \text{TOL}$, then stop. Otherwise, $k \leftarrow k + 1$, and go to step 1.
-

4.5 Integrating over unfitted domains

The computation of $\int_{\Omega^i(u)} \phi(t_i, \cdot) d\mathbf{x}$ over a discrete, unfitted grid is problematic. A simple method, that avoids dealing with mesh intersections, could be to define a smoothed characteristic function χ^i that represents Ω^i , or project the smooth characteristic onto piecewise constant functions over the background grid \mathcal{T}_h . Then, simply replace $\int_{\Omega^i(u)} \phi(t_i, \cdot) d\mathbf{x}$ with

$$\int_{\mathcal{D}} \chi^i \phi(t_i, \cdot) d\mathbf{x},$$

and integrate in a standard way over \mathcal{T}_h . However, the accuracy of this approach could be an issue.

Hence, we opted for the following approach, which still avoids mesh intersections but incurs some additional computational cost. For each i , let $\boldsymbol{\sigma}^i \in \mathbb{S}_h^2 \subset [H^1(\mathcal{D})]^n$ be a piecewise quadratic vector field such that

$$\begin{aligned} \operatorname{div} \boldsymbol{\sigma}^i(\cdot) &= \phi(t_i, \cdot), & \text{in } \mathcal{D}, \\ \boldsymbol{\sigma}^i &= \mathbf{0}, & \text{on } \partial\mathcal{D}, \end{aligned} \quad (59)$$

We implement this construction by solving a discrete Stokes problem with standard Taylor-Hood elements. Since the level set function is predetermined, this can be done offline. Then, we can make the following approximation:

$$\int_{\Omega^i} \phi(t_i, \cdot) d\mathbf{x} = \int_{\Omega^i} \operatorname{div} \boldsymbol{\sigma}^i d\mathbf{x} = \int_{\Gamma^i} \boldsymbol{\sigma}^i \cdot \boldsymbol{\nu} dS(\mathbf{x}) \approx \int_{\Gamma^i} (\pi_h^i \boldsymbol{\sigma}^i) \cdot \boldsymbol{\nu} dS(\mathbf{x}). \quad (60)$$

Thus, the only geometric approximation error is due to interpolating σ onto Γ^i . We apply the same approach for computing the “energy” of Γ^i in the gradient flow of the forward problem as it depends on the control u integrated over Ω^i .

5 Numerical results

We present examples in two and three dimensions. In both cases, we seek a time-independent control that drives Γ^t toward a desired non-convex shape at the final time t_f . All computations were done using the Matlab/C++ FEM toolbox FELICITY [36]. All 3-D linear system solves use the algebraic multi-grid solver (AGMG) [27, 25, 26, 28]; the Stokes system is solved using the method in [29, 30]. All 2-D solves simply use the “backslash” command in Matlab.

5.1 Two-dimensional T-Shape

This example seeks to find u such that the curve Γ evolves toward a T-shape. The time-independent level set function is given by

$$\phi(x, y) = \widetilde{\min} \left(\max(|x + 0.60| - 0.05, 0)^2 + \max(|y| - 0.8, 0)^2 - (0.2)^2, \right. \\ \left. \max(|x + 0.25| - 1.05, 0)^2 + \max(|y - 0.75| - 0.05, 0)^2 - (0.2)^2 \right), \quad (61)$$

where $\widetilde{\min}(a, b) := (a + b)/2 - |a - b|_\epsilon/2$ and $|s|_\epsilon := \sqrt{s^2 + \epsilon^2}$ with $\epsilon = 0.02$. For the forward problem, the time interval is $[0, t_f]$ with $t_f = 3$ and $N = 100$ time steps. The initial curve Γ^0 is specified to be a circle of radius 0.81. In addition, we used a piecewise quadratic approximation of the curve for the method in (49), with 200 edges in the mesh.

The optimization parameters are as follows. The “hold-all” domain is $\mathfrak{D} = [-2, 2]^2$, $\alpha = 10^{-4}$, discretized with a uniform triangular mesh consisting of 20201 vertices, and 40000 triangles. The inner product $a(\cdot, \cdot)$ in (57) is given by

$$a(\eta, \xi) = \int_{\mathfrak{D}} \eta \xi \, d\mathbf{x} + \beta \int_{\mathfrak{D}} \nabla \eta \cdot \nabla \xi \, d\mathbf{x}, \quad (62)$$

where $\beta = 0.1$. The initial guess for u is simply $u_0 \equiv 0$, which causes Γ to remain a circle for all time.

Figure 2 shows how the control u is updated by the optimization. Clearly, the control is chosen to drive Γ to the desired shape represented by the black curve. A plot of the objective functional cost (56) is shown in Figure 3.

Figure 4 shows the evolution of the forward simulation using the control obtained at the final optimization iteration. Figure 5 shows the “energy” of the forward simulation versus time, where the energy is defined by (4).

Figure 6 shows the evolution of Γ with a perturbed initial circle, i.e. the center of the circle is $(0.02, 0.0)$. Here, Γ does *not* converge toward the desired shape. However, using an initial center of $(0.01, 0.0)$ yields an evolution similar to Figure 4. Figure 7 shows the case where the initial circle center is $(0.0, -0.02)$. Again, Γ does *not* converge toward the desired shape, but using an initial center of $(0.0, -0.01)$ yields an evolution similar to Figure 4. Hence, the optimal control found is sensitive to perturbations of the initial condition.

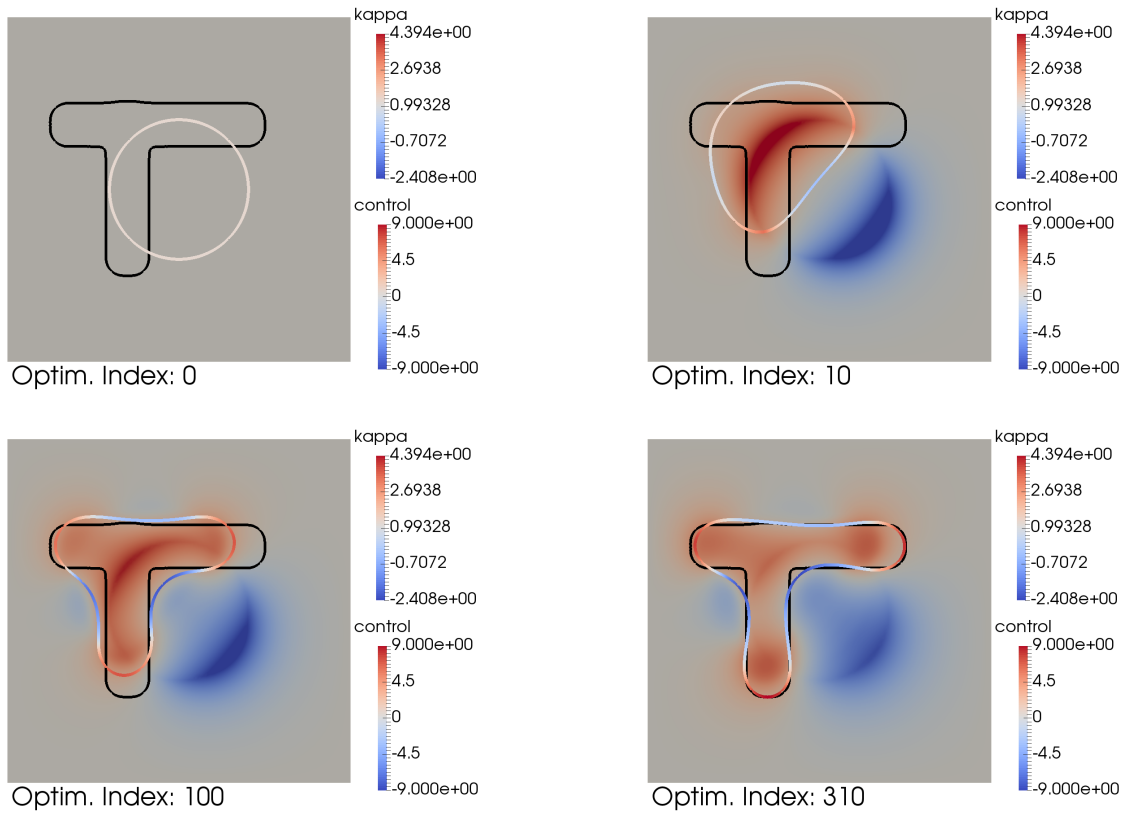


Figure 2: Evolution of the control u versus optimization iteration (Section 5.1). The black curve is the zero level set of ϕ . The curve Γ is plotted (at the final time of the forward simulation) with color according to κ (the additive curvature). The background control function u is plotted with its own color scale.

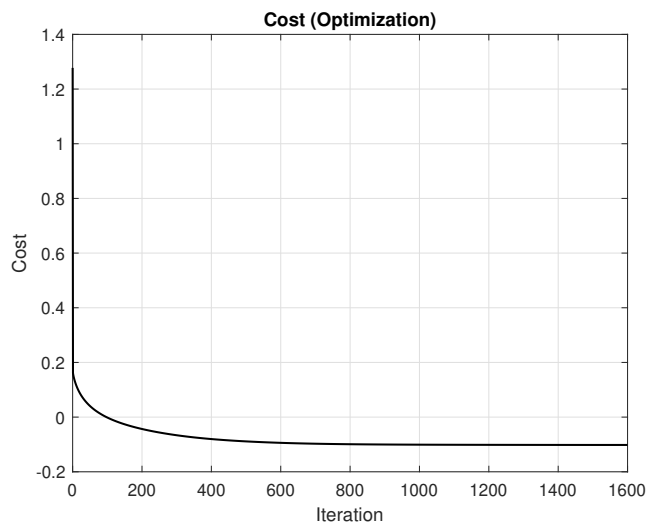


Figure 3: Decrease of the optimization cost (56) versus optimization iteration (Section 5.1).

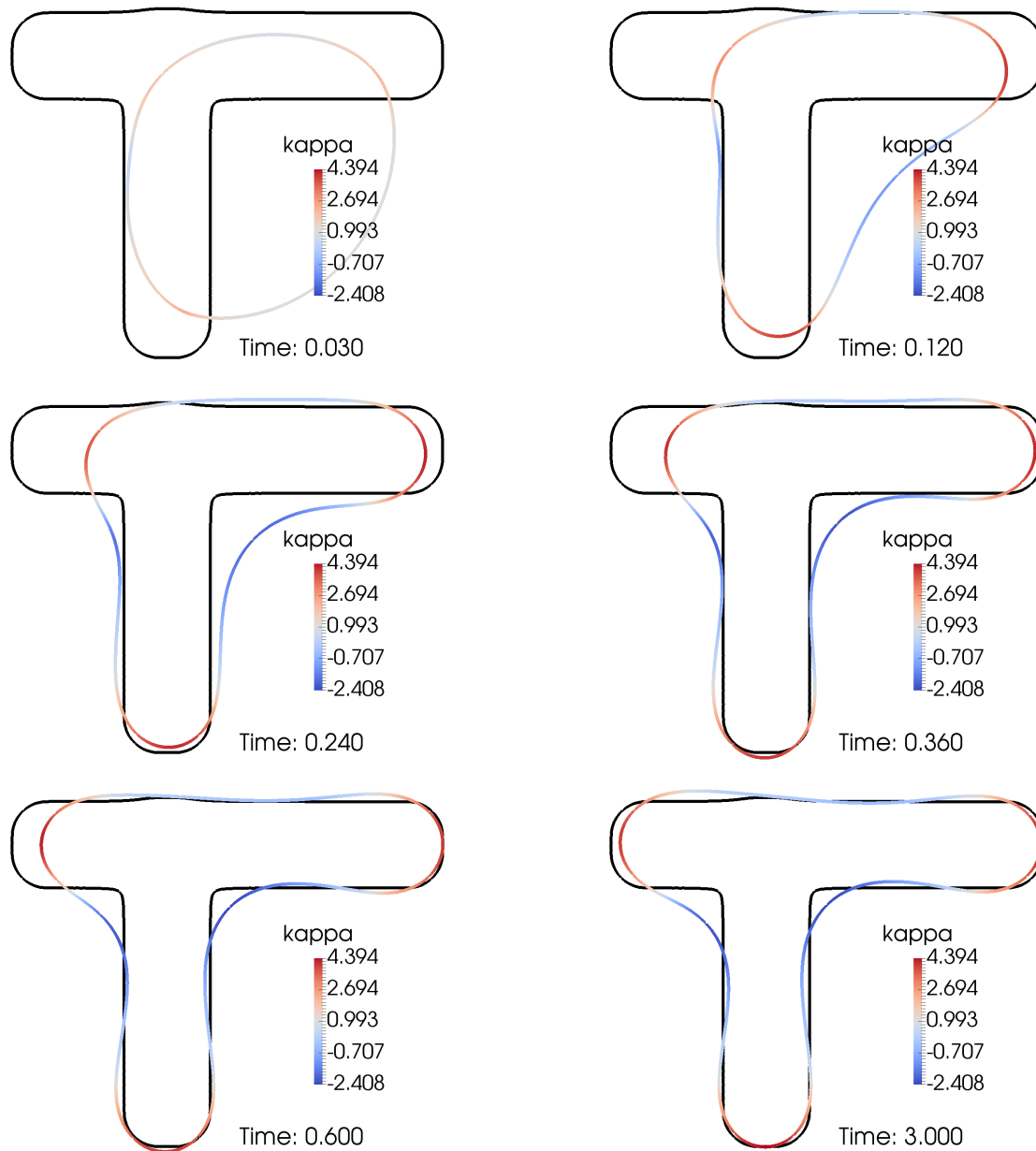


Figure 4: Evolution of the forward simulation using the final control obtained by the optimization (Section 5.1). The black curve is the zero level set of ϕ . The curve Γ is plotted with color according to κ .

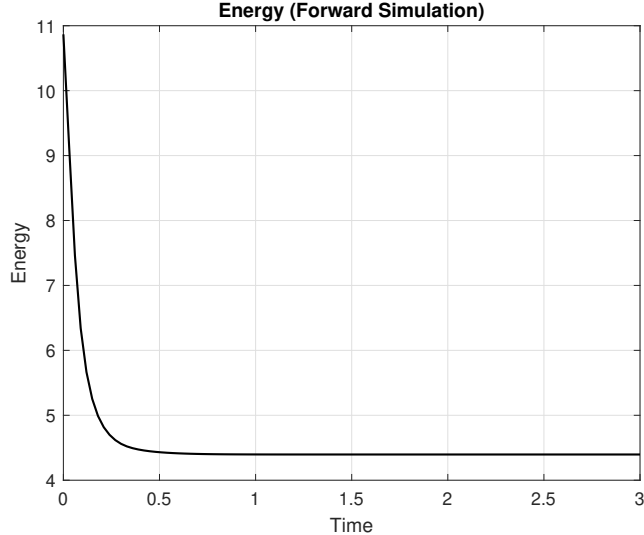


Figure 5: Energy (4) of the forward simulation versus time (Section 5.1). The control obtained at the final optimization iteration is used here.

5.2 Two-dimensional Dumbbell

This example seeks to find u such that the curve Γ evolves toward a dumbbell shape. The time-independent level set function is given by

$$\phi(x, y) = 2.4 - \sum_{i=1}^2 \left[\left(\frac{x}{1.35} + a_i \right)^2 + \left(\frac{y}{1.35} + b_i \right)^2 + 0.1 \right]^{-1/2}, \quad (63)$$

where $a_1 = -0.75$, $a_2 = +0.75$, $b_1 = 0.0$, $b_2 = 0.0$. For the forward problem, the time interval is $[0, t_f]$ with $t_f = 1$ and $N = 60$ time steps. The initial curve Γ^0 is specified to be a circle of radius 1.0. In addition, we used a piecewise quadratic approximation of the curve for the method in (49), with 100 edges in the mesh.

The optimization parameters are as follows. The “hold-all” domain is $\mathfrak{D} = [-2, 2]^2$, $\alpha = 10^{-4}$, discretized with a uniform triangular mesh consisting of 7321 vertices, and 14400 triangles. The inner product $a(\cdot, \cdot)$ in (57) is given by (62). The initial guess for u is simply $u_0 \equiv 0$, which causes Γ to remain a circle for all time.

Figure 8 shows how the control u is updated by the optimization. Clearly, the control is chosen to drive Γ to the desired shape represented by the black curve. A plot of the objective functional cost (56) is shown in Figure 9.

Figure 10 shows the evolution of the forward simulation using the control obtained at the final optimization iteration. Figure 11 shows the “energy” of the forward simulation versus time, where the energy is defined by (4).

Figure 12 shows the evolution of Γ with a perturbed initial circle, i.e. the center of the circle is $(0.2, 0.0)$. Figure 13 shows the case where the initial circle center is $(0.3, 0.3)$. Hence, the optimal control found appears to be somewhat robust to perturbations of the initial condition. Of course, a sufficiently large perturbation will cause the curve to evolve to a circle *outside* of the zero level set.

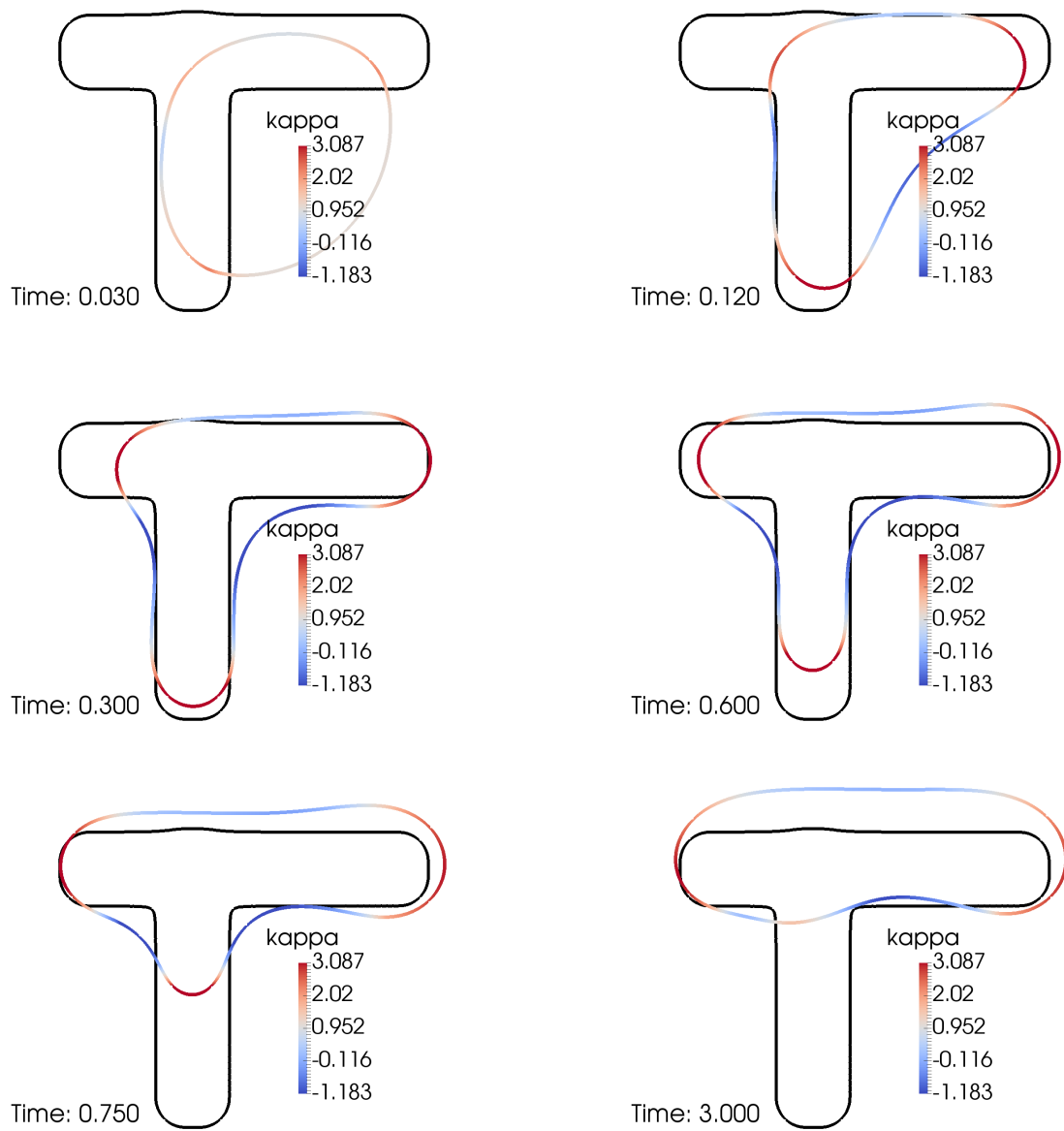


Figure 6: Evolution of the forward simulation with perturbed initial circle with center at $(0.02, 0.0)$ (Section 5.1). The control u was taken from the final iteration of the optimization.

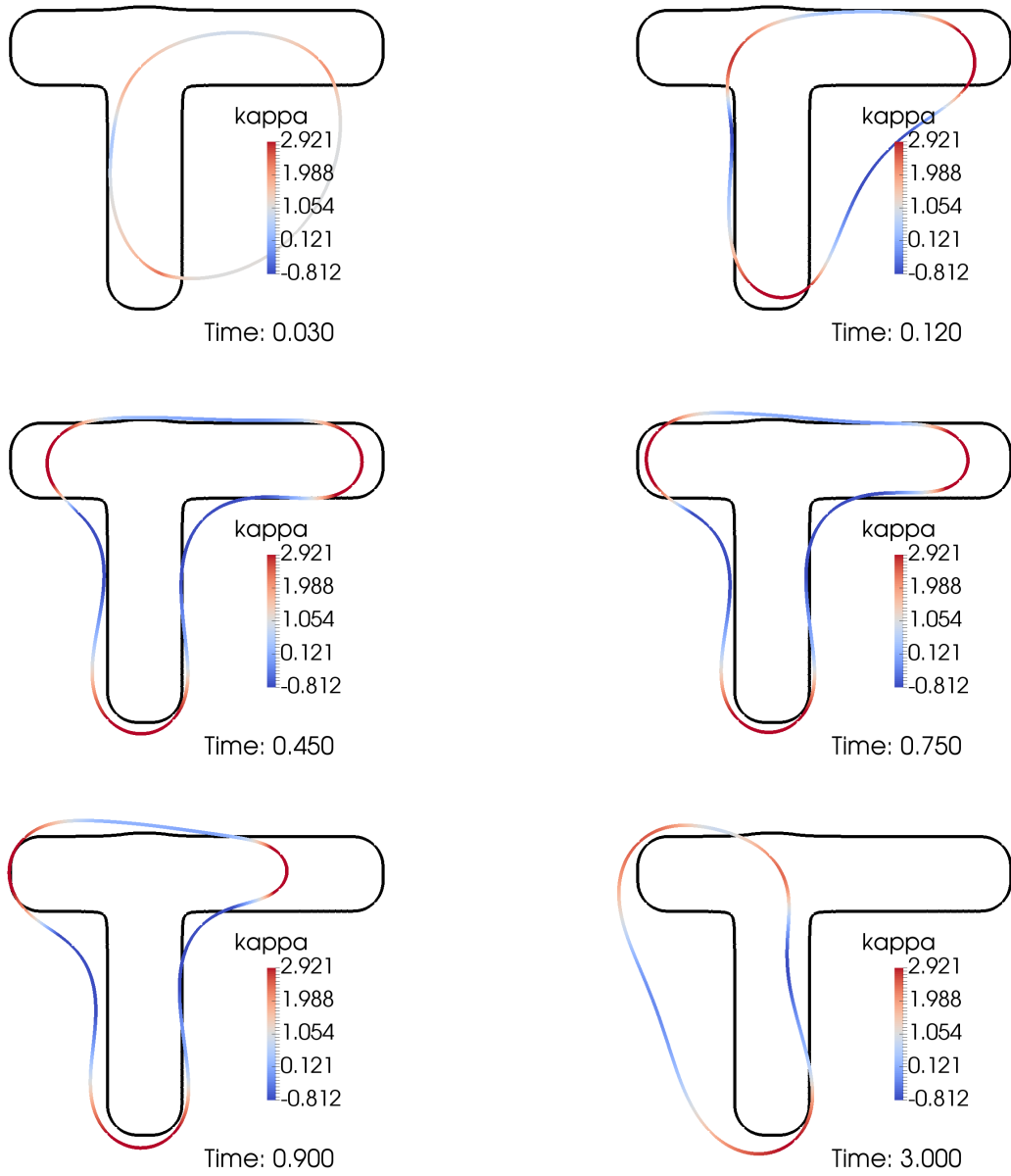


Figure 7: Evolution of the forward simulation with perturbed initial circle with center at $(0.0, -0.02)$ (Section 5.1). The control u was taken from the final iteration of the optimization.

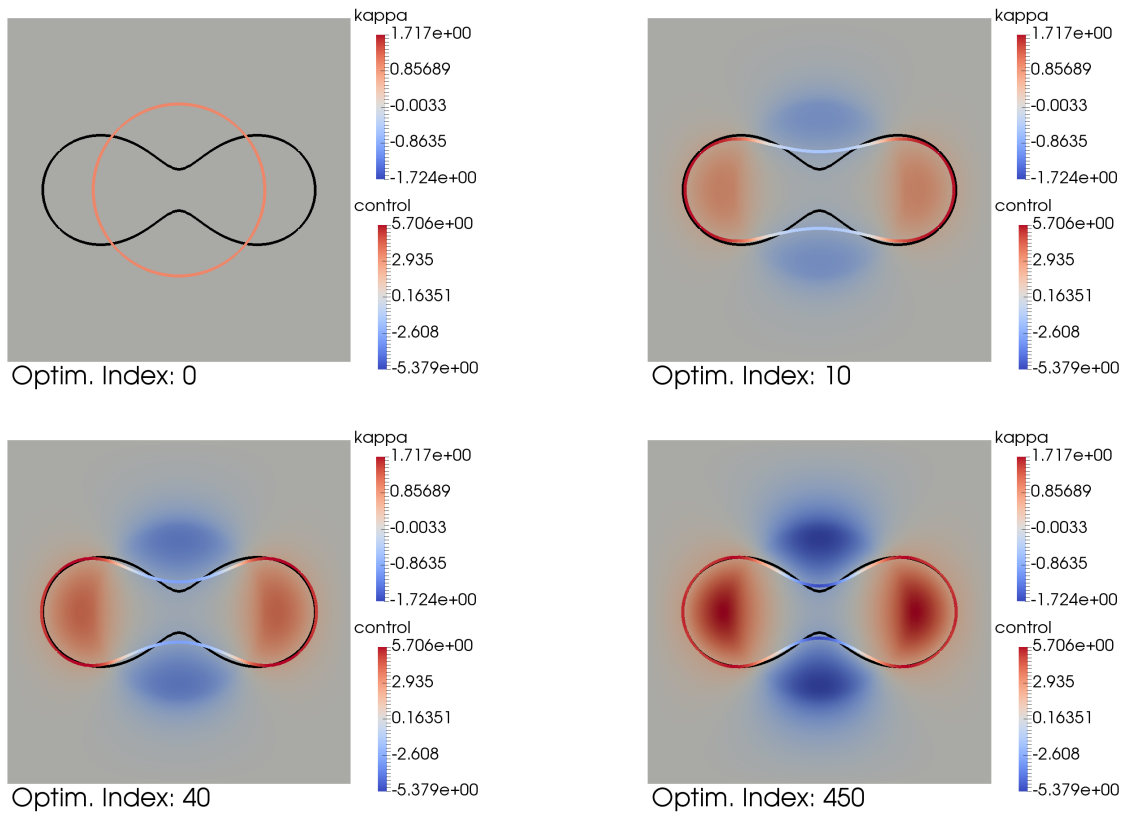


Figure 8: Evolution of the control u versus optimization iteration (Section 5.2). The black curve is the zero level set of ϕ . The curve Γ is plotted (at the final time of the forward simulation) with color according to κ (the additive curvature). The background control function u is plotted with its own color scale.

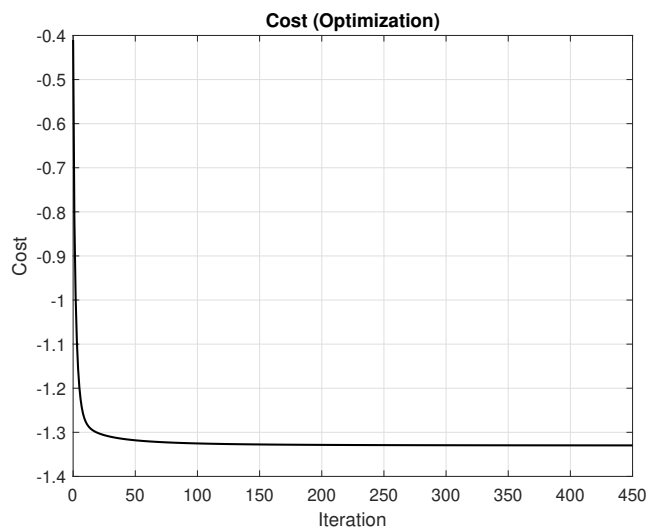


Figure 9: Decrease of the optimization cost (56) versus optimization iteration (Section 5.2).

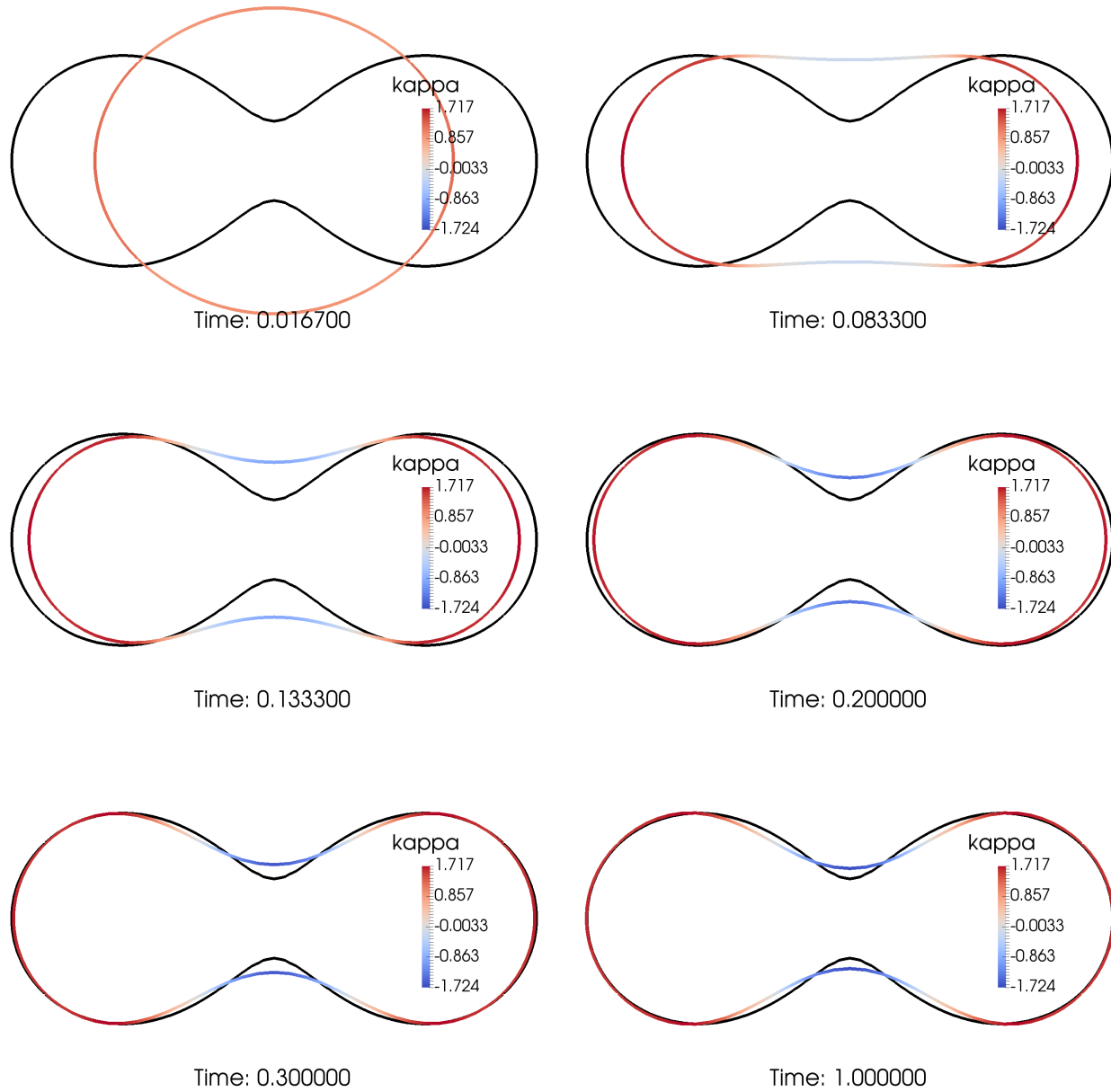


Figure 10: Evolution of the forward simulation using the final control obtained by the optimization (Section 5.2). The black curve is the zero level set of ϕ . The curve Γ is plotted with color according to κ .

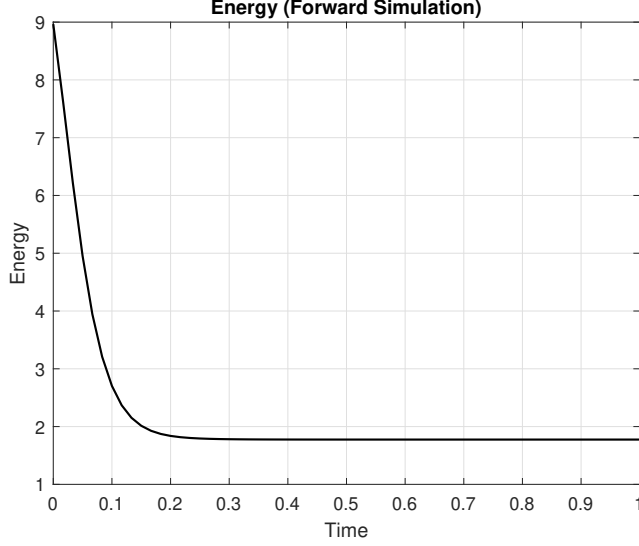


Figure 11: Energy (4) of the forward simulation versus time (Section 5.2). The control obtained at the final optimization iteration is used here.

5.3 Three-dimensional Dumbbell

This example seeks to find u such that the surface Γ evolves toward a dumbbell shape. The time-independent level set function is given by

$$\phi(x, y, z) = 2.4 - \sum_{i=1}^2 \left[\left(\frac{x}{1.52} + a_i \right)^2 + \left(\frac{y}{1.52} + b_i \right)^2 + \left(\frac{z}{1.52} + c_i \right)^2 + 0.1 \right]^{-1/2}, \quad (64)$$

where $a_1 = -0.75$, $a_2 = +0.75$, $b_1 = 0.0$, $b_2 = 0.0$, $c_1 = 0.0$, $c_2 = 0.0$ (Figure 14 illustrates the zero level set of (64)). For the forward problem, the time interval is $[0, t_f]$ with $t_f = 1$ and $N = 10$ time steps. The initial surface Γ^0 is specified to be a sphere of radius 1.0. In addition, we used a piecewise quadratic triangular surface mesh for the method in (49), with 2048 triangles and 1026 vertices.

The optimization parameters are as follows. The “hold-all” domain is $\mathfrak{D} = [-2.5, 2.5]^3$, $\alpha = 10^{-4}$, discretized with a uniform tetrahedral mesh consisting of 137720 vertices, and 768000 tetrahedra. The inner product $a(\cdot, \cdot)$ in (57) is similar to (62), where $\beta = 0.1$. The initial guess for u is simply $u_0 \equiv 0$, which causes Γ to remain a sphere for all time.

Figure 15 shows how Γ^{t_f} changes based on the optimization iteration, while Figure 16 shows how the control u is updated by the optimization. Clearly, the control is chosen to drive Γ to the desired shape (see the white surface/curve). A plot of the objective functional cost (56) is shown in Figure 17.

Figure 18 shows the evolution of the forward simulation using the control obtained at the final optimization iteration. Figure 19 shows the “energy” of the forward simulation versus time.

Figure 20 shows the evolution of Γ with a perturbed initial sphere, i.e. the center of the sphere is $(0.2, 0.0, 0.0)$. Figure 21 shows the case where the initial sphere center is $(0.22, 0.22, 0.22)$. Hence, the optimal control found appears to be somewhat robust to perturbations of the initial condition. Of course, a sufficiently large perturbation will cause the sphere to evolve to a sphere *outside* of the zero level set.

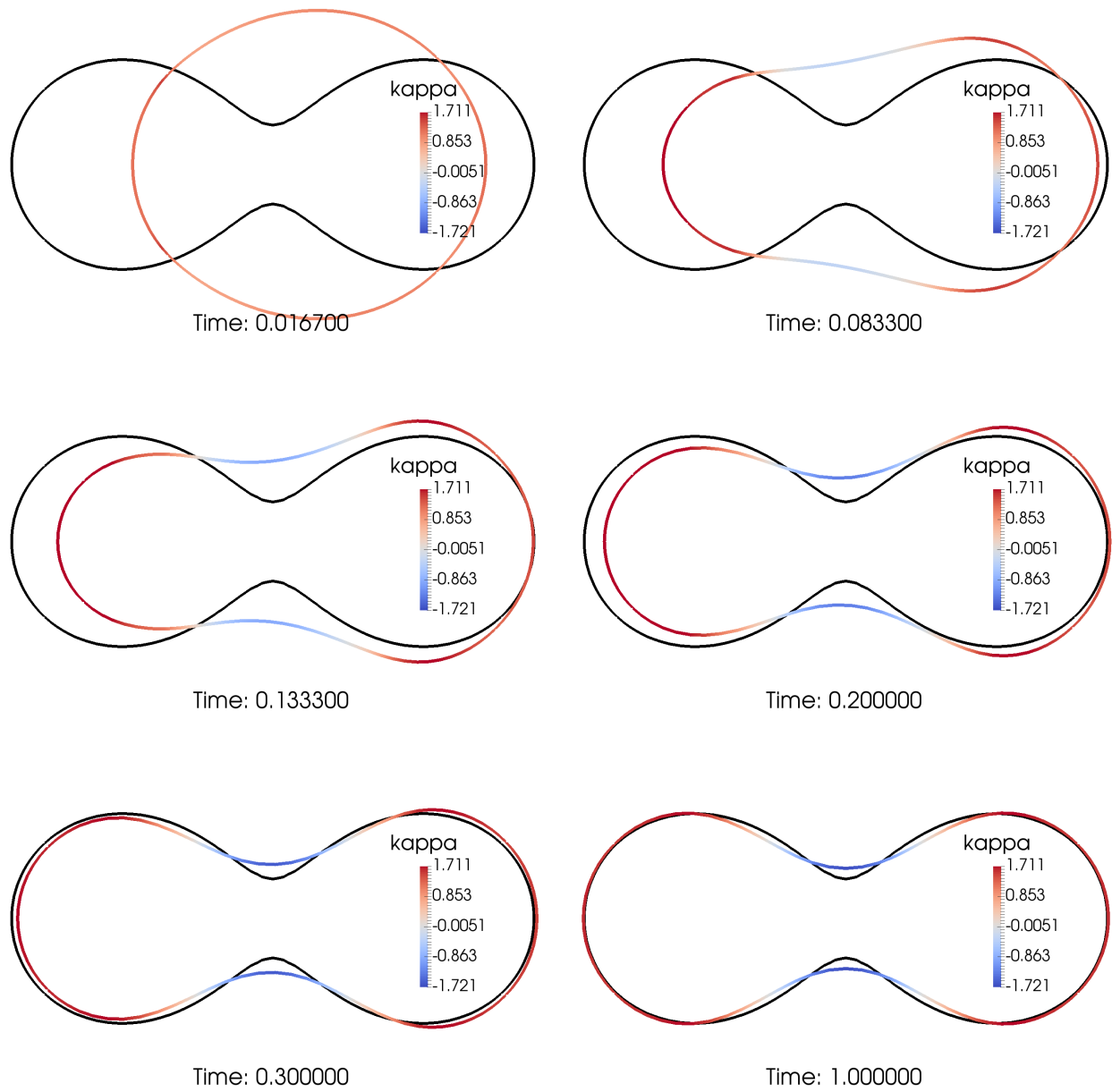


Figure 12: Evolution of the forward simulation with perturbed initial circle with center at $(0.2, 0.0)$ (Section 5.2). The control u was taken from the final iteration of the optimization.

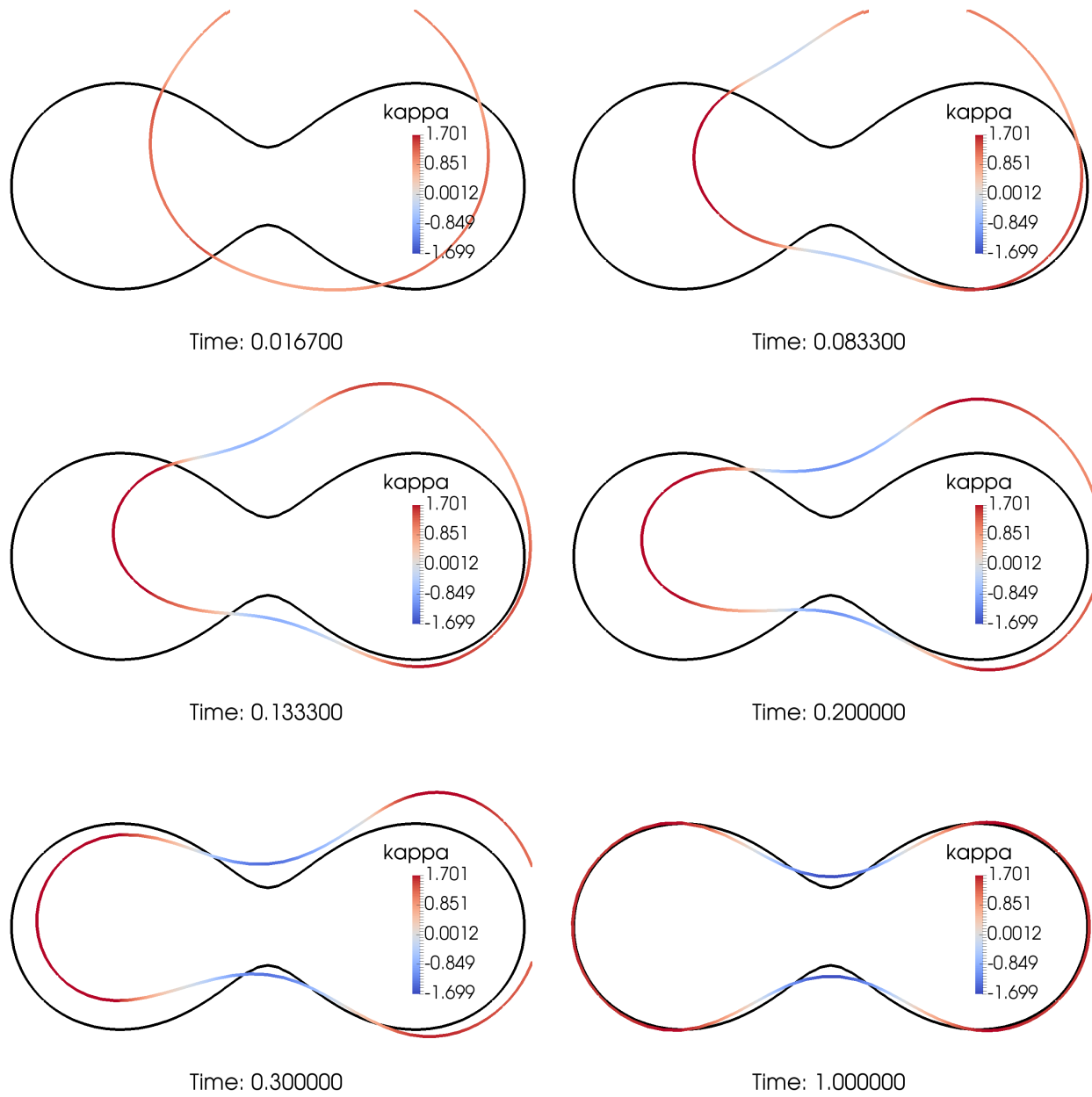


Figure 13: Evolution of the forward simulation with perturbed initial circle with center at $(0.3, 0.3)$ (Section 5.2). The control u was taken from the final iteration of the optimization.

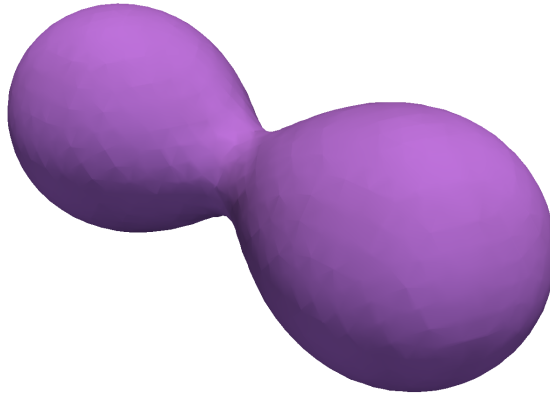


Figure 14: Illustration of the zero level set of (64) (Section 5.3).

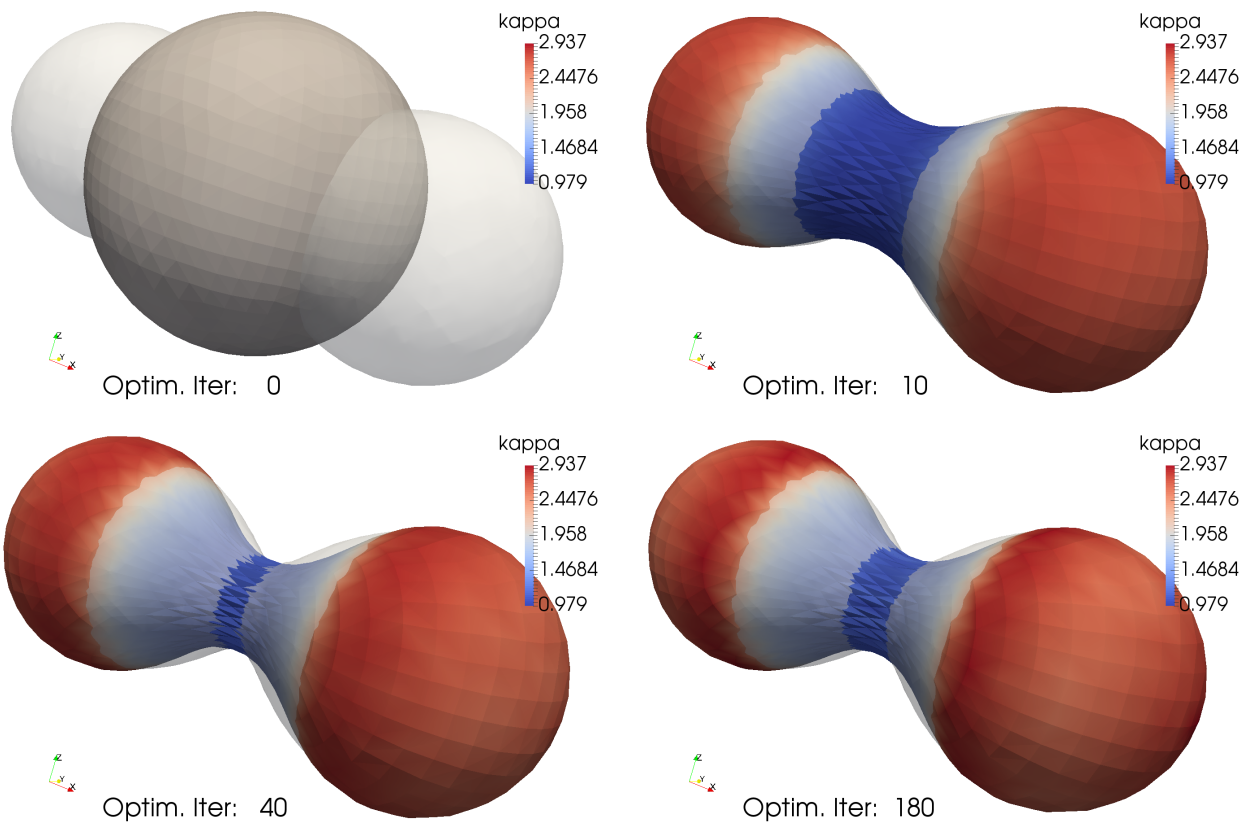


Figure 15: Evolution of Γ^{t_f} versus optimization iteration (Section 5.3). The white (transparent) surface is the zero level set of ϕ . The surface Γ is plotted (at the final time of the forward simulation) with color according to κ (the additive curvature). Note that the coloring is affected by the transparent zero level set.

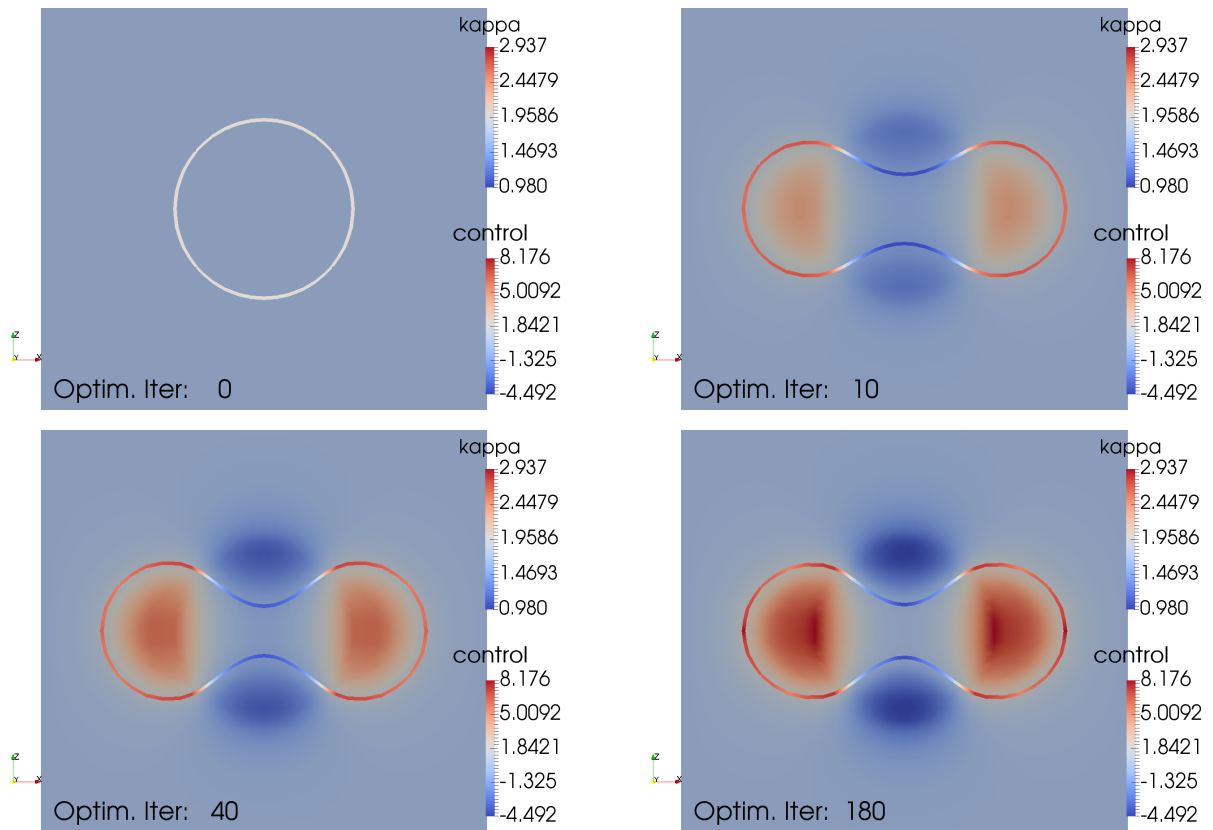


Figure 16: Evolution of the control u versus optimization iteration (Section 5.3); a 2-D slice is shown. The white curve is the zero level set of ϕ . The slice of Γ , which is a curve, is plotted (at the final time of the forward simulation) with color according to κ . The background control function u is plotted with its own color scale.

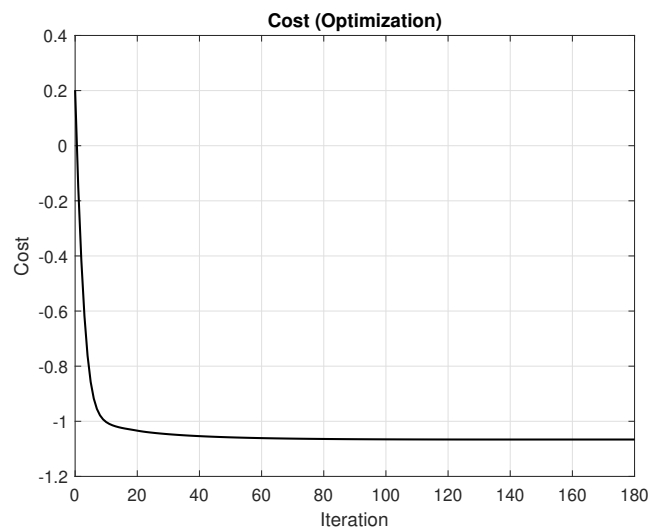


Figure 17: Decrease of the optimization cost (56) versus optimization iteration (Section 5.3).

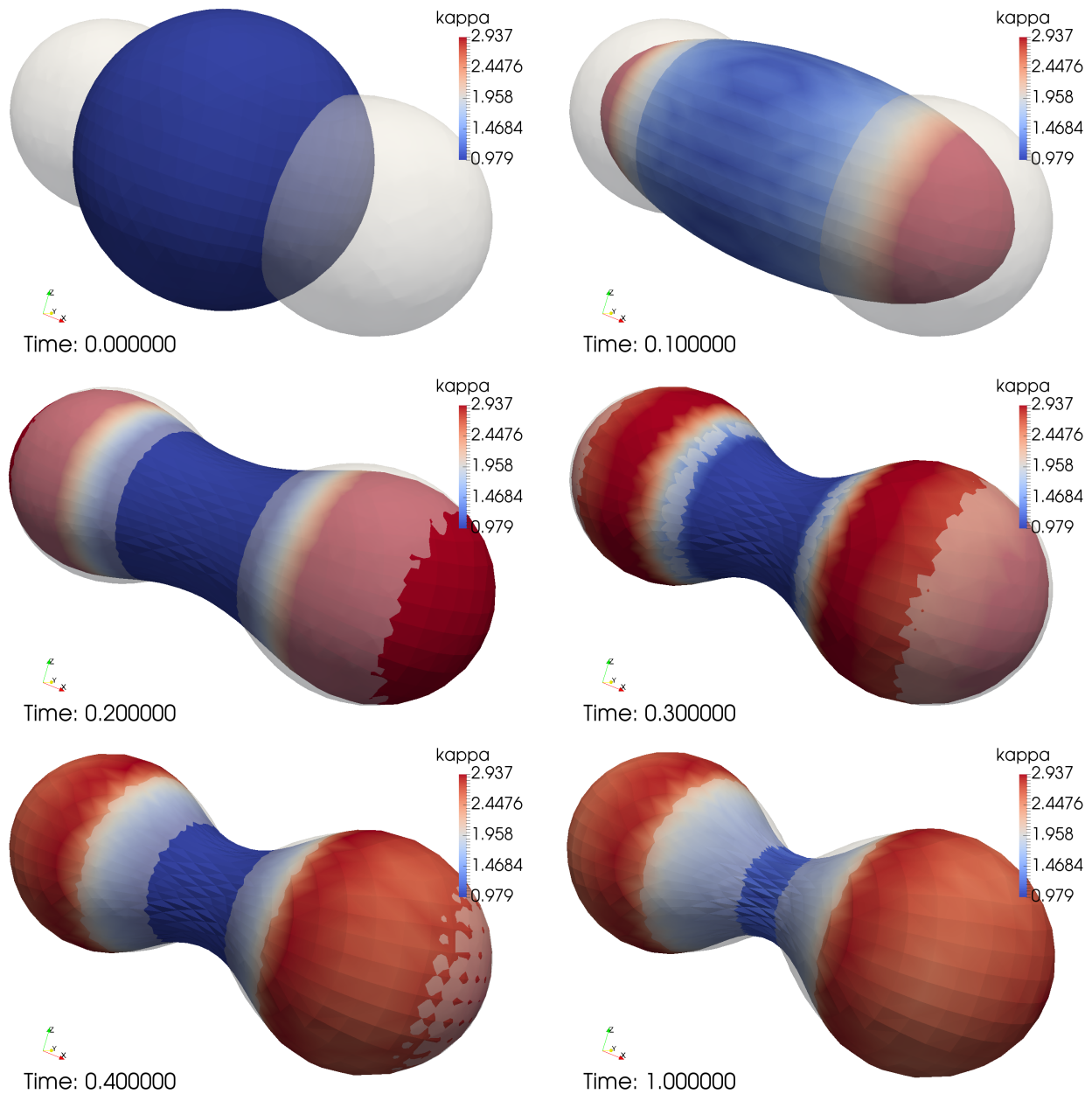


Figure 18: Evolution of the forward simulation using the final control obtained by the optimization (Section 5.3). The white (transparent) surface is the zero level set of ϕ . The surface Γ is plotted with color according to κ (the additive curvature).

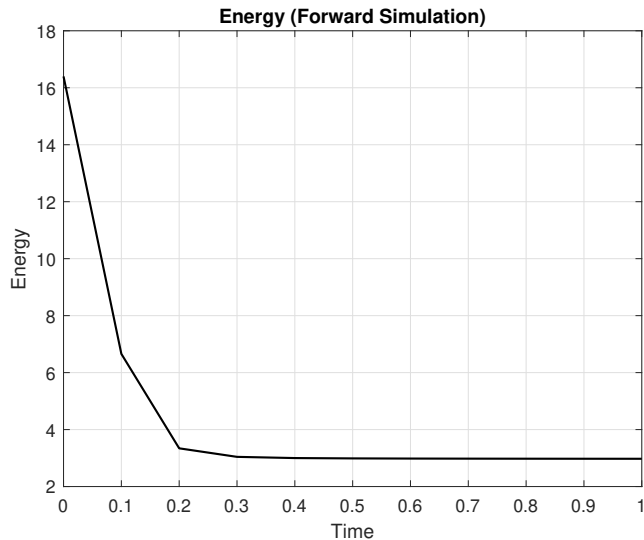


Figure 19: Energy (4) of the forward simulation versus time (Section 5.3). The control obtained at the final optimization iteration is used here.

6 Conclusion

We have developed a methodology for doing optimal PDE control of geometrically driven flows. A central concept in the method is the *transverse field* which accounts for the evolution of the domain and appears in the sensitivity analysis with respect to perturbations of the corresponding space-time tube. An important contribution of the paper is the introduction of an *adjoint transverse field* to compute the derivative of the cost functional, appearing as the solution of a backwards parabolic equation with terminal conditions on the boundary of the space-time tube. In this way, we extend the usual adjoint calculus from PDE-constrained optimization to optimal control of gradient flows. As a test problem, we consider optimal control of the mean curvature flow equation with volume constraint via a forcing term. The methodology is general and the derivation we present can be extended to incorporate other geometrically driven flows.

Furthermore, we present an effective numerical scheme that captures the geometric evolution of the (forward) problem with reasonable efficiency, as well as a discrete optimization method for finding an optimal control that minimizes our tracking type objective functional. We also demonstrated that our optimal control results can be sensitive to initial perturbations of the forward problem. In other cases, the results are reasonably robust. The sensitivity is probably linked to the complexity of the desired shape. Improving the robustness of the control, through modification of the optimization scheme, will be a topic for further investigation.

Several questions remain, however, about this framework. Proving rigorous differentiability results about the forward problem, with respect to the control, appears to be extremely challenging as it would require advanced regularity results about PDEs on moving surfaces as well as geometric and regularity properties of general gradient flows, which are still active research topics. It is also not clear what are the “reachable states” of the forward problem, i.e. what kind of stationary states can we drive the evolution toward? Our numerical results indicate that regions with high curvature or geometric singularities may be difficult or impossible to reach. In addition, there are many open numerical questions, such as convergence of the forward problem and of the optimal control.

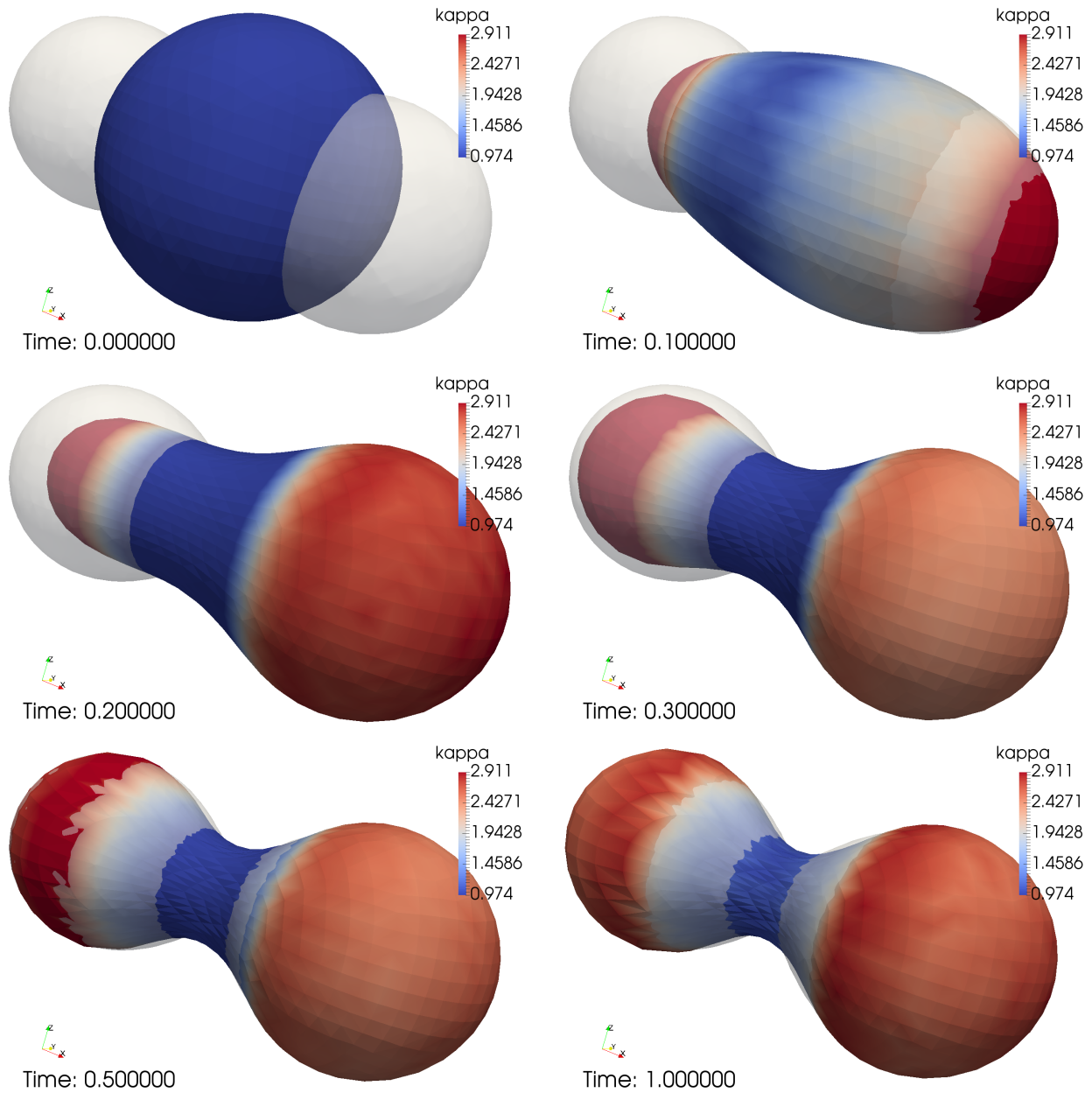


Figure 20: Evolution of the forward simulation with perturbed initial sphere with center at $(0.2, 0.0, 0.0)$ (Section 5.3). The control u was taken from the final iteration of the optimization.

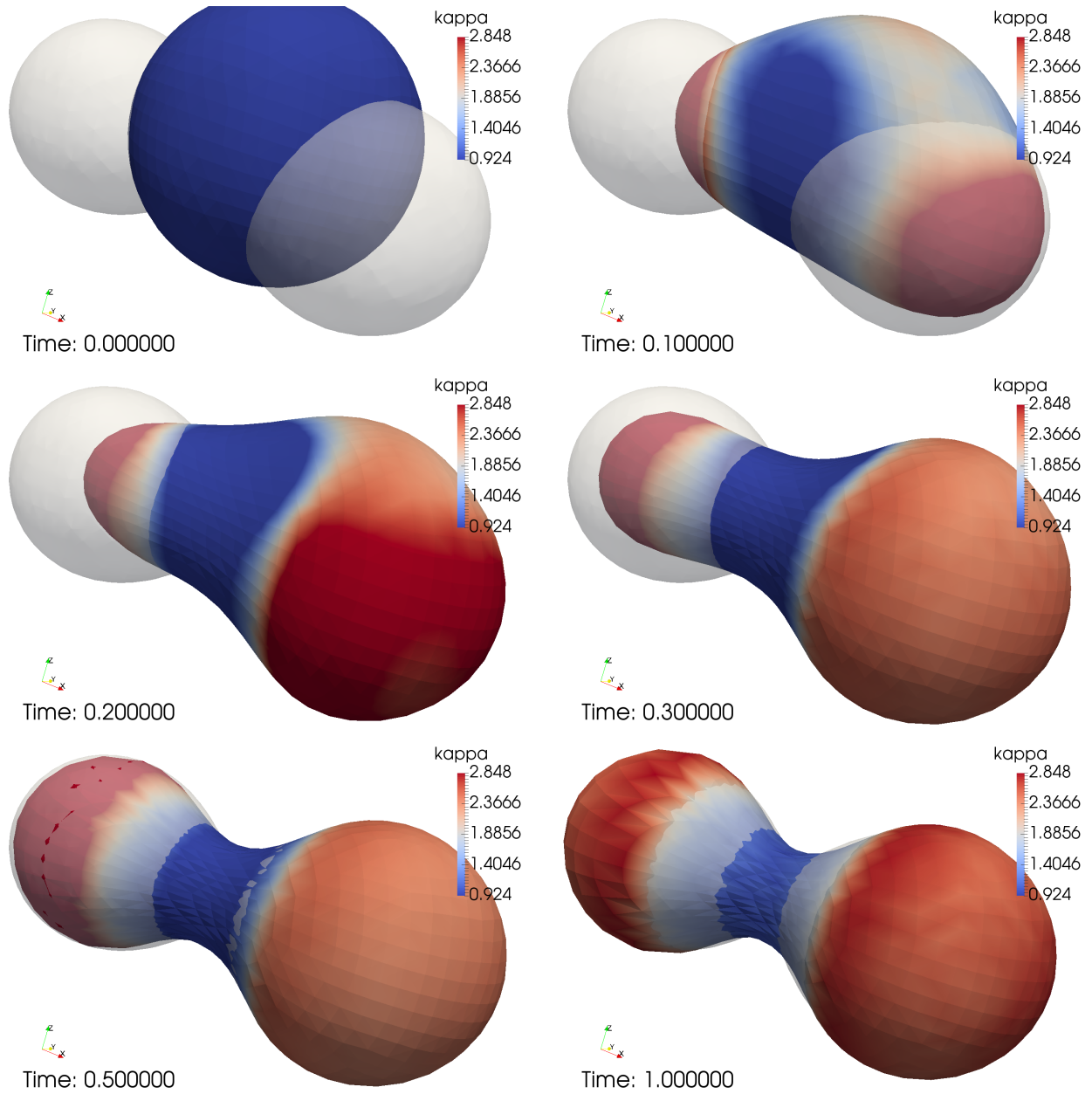


Figure 21: Evolution of the forward simulation with perturbed initial sphere with center at $(0.22, 0.22, 0.22)$ (Section 5.3). The control u was taken from the final iteration of the optimization.

Acknowledgements

Antoine Laurain gratefully acknowledges the support of the Brazilian National Council for Scientific and Technological Development (Conselho Nacional de Desenvolvimento Científico e Tecnológico - CNPq) through the process: 408175/2018-4 “Otimização de forma não suave e controle de problemas de fronteira livre”, and through the program “Bolsa de Produtividade em Pesquisa - PQ 2018”, process: 304258/2018-0. Shawn W. Walker acknowledges financial support by the National Science Foundation (NSF) via DMS-1555222 (CAREER).

A Appendix

A.1 Identities

Lemma 1. *Let $\Gamma \subset \mathbb{R}^n$ be a $(n - 1)$ -dimensional manifold without boundary. Then we have for sufficiently smooth functions $v, w : \Gamma \rightarrow \mathbb{R}$,*

$$\int_{\Gamma} w \Delta_{\Gamma} v - v \Delta_{\Gamma} w = \int_{\Gamma} (\nabla_{\Gamma} v \cdot \mathbf{b}) w - (\nabla_{\Gamma} w \cdot \mathbf{b}) v. \quad (65)$$

Proof. We have

$$\begin{aligned} \int_{\Gamma} w \Delta_{\Gamma} v - v \Delta_{\Gamma} w &= \int_{\Gamma} \operatorname{div}_{\Gamma} (w \nabla_{\Gamma} v - v \nabla_{\Gamma} w) \\ &= \int_{\Gamma} \kappa (w \nabla_{\Gamma} v - v \nabla_{\Gamma} w) \cdot \boldsymbol{\nu} + \int_{\Gamma} (\nabla_{\Gamma} v \cdot \mathbf{b}) w - (\nabla_{\Gamma} w \cdot \mathbf{b}) v, \end{aligned}$$

which yields the result. \square

References

- [1] A. Alphonse, C. M. Elliott, and B. Stinner. An abstract framework for parabolic PDEs on evolving spaces. *Port. Math.*, 72(1):1–46, 2015.
- [2] A. Alphonse, C. M. Elliott, and B. Stinner. On some linear parabolic PDEs on moving hypersurfaces. *Interfaces Free Bound.*, 17(2):157–187, 2015.
- [3] B. Andrews. Volume-preserving anisotropic mean curvature flow. *Indiana Univ. Math. J.*, 50(2):783–827, 2001.
- [4] S. Angenent. Parabolic equations for curves on surfaces. I. Curves with p -integrable curvature. *Ann. of Math. (2)*, 132(3):451–483, 1990.
- [5] S. Angenent. Parabolic equations for curves on surfaces. II. Intersections, blow-up and generalized solutions. *Ann. of Math. (2)*, 133(1):171–215, 1991.
- [6] M. Astorino, J.-F. Gerbeau, O. Pantz, and K.-F. Traoré. Fluidstructure interaction and multi-body contact: Application to aortic valves. *Computer Methods in Applied Mechanics and Engineering*, 198(45):3603 – 3612, 2009. Models and Methods in Computational Vascular and Cardiovascular Mechanics.
- [7] G. Barles, H. M. Soner, and P. E. Souganidis. Front propagation and phase field theory. *SIAM J. Control Optim.*, 31(2):439–469, 1993.

- [8] J. W. Barrett, H. Garcke, and R. Nürnberg. A parametric finite element method for fourth order geometric evolution equations. *Journal of Computational Physics*, 222(1):441 – 467, 2007.
- [9] J. W. Barrett, H. Garcke, and R. Nürnberg. A variational formulation of anisotropic geometric evolution equations in higher dimensions. *Numerische Mathematik*, 109(1):1–44, 2008.
- [10] A. Chambolle and M. Novaga. Implicit time discretization of the mean curvature flow with a discontinuous forcing term. *Interfaces and Free Boundaries*, pages 283–300, 2008.
- [11] A. Chicco-Ruiz, P. Morin, and M. S. Pauletti. The shape derivative of the gauss curvature. *Revista de la Unión Matemática Argentina*, pages 311–337, May 2018.
- [12] M. C. Delfour and J.-P. Zolésio. *Shapes and Geometries: Analysis, Differential Calculus, and Optimization*, volume 4 of *Advances in Design and Control*. SIAM, 2nd edition, 2011.
- [13] R. Dziri and J.-P. Zolésio. *Shape Optimization and Optimal Design*, chapter Eulerian Derivative for Non-Cylindrical Functionals, pages 87–107. Lecture Notes in Pure and Applied Mathematics. Dekker, New York, 2001.
- [14] Y. Giga. *Surface evolution equations*, volume 99 of *Monographs in Mathematics*. Birkhäuser Verlag, Basel, 2006. A level set approach.
- [15] A. Henrot and M. Pierre. *Shape variation and optimization*, volume 28 of *EMS Tracts in Mathematics*. European Mathematical Society (EMS), Zürich, 2018. A geometrical analysis, English version of the French publication [MR2512810] with additions and updates.
- [16] M. Hintermüller and A. Laurain. Optimal shape design subject to elliptic variational inequalities. *SIAM J. Control Optim.*, 49(3):1015–1047, 2011.
- [17] H. Kasumba, K. Kunisch, and A. Laurain. A bilevel shape optimization problem for the exterior Bernoulli free boundary value problem. *Interfaces Free Bound.*, 16(4):459–487, 2014.
- [18] I. Kim and D. Kwon. On mean curvature flow with forcing. *Communications in Partial Differential Equations*, 45(5):414–455, Dec. 2019.
- [19] I. Kim and D. Kwon. Volume preserving mean curvature flow for star-shaped sets. *Calc. Var. Partial Differential Equations*, 59(2):Paper No. 81, 40, 2020.
- [20] B. Kovács and C. Lubich. Linearly implicit full discretization of surface evolution. *Numerische Mathematik*, 140(1):121–152, Mar. 2018.
- [21] A. Laurain and S. W. Walker. Droplet footprint control. *SIAM Journal on Control and Optimization*, 53(2):771–799, 2015.
- [22] P. Le Tallec, J.-F. Gerbeau, P. Hauret, and M. Vidrascu. Fluid structure interaction problems in large deformation. *Comptes Rendus Mécanique*, 333(12):910 – 922, 2005. Fluid-solid interactions: modeling, simulation, bio-mechanical applications.
- [23] U. F. Mayer. A singular example for the averaged mean curvature flow. *Experiment. Math.*, 10(1):103–107, 2001.
- [24] M. Moubachir and J.-P. Zolésio. *Moving Shape Analysis and Control: Applications to Fluid Structure Interactions*, volume 277 of *Pure and Applied Mathematics*. Chapman and Hall/CRC, 2006.

- [25] A. Napov and Y. Notay. Algebraic analysis of aggregation-based multigrid. *Numerical Linear Algebra with Applications*, 18(3):539–564, 2011.
- [26] A. Napov and Y. Notay. An algebraic multigrid method with guaranteed convergence rate. *SIAM Journal on Scientific Computing*, 34(2):A1079–A1109, 2012.
- [27] Y. Notay. An aggregation-based algebraic multigrid method. *Electronic Transactions On Numerical Analysis*, 37:123–146, 2010.
- [28] Y. Notay. Aggregation-based algebraic multigrid for convection-diffusion equations. *SIAM Journal on Scientific Computing*, 34(4):A2288–A2316, 2012.
- [29] Y. Notay. A new algebraic multigrid approach for stokes problems. *Numerische Mathematik*, 132:51–84, 2016.
- [30] Y. Notay. Algebraic multigrid for stokes equations. *SIAM Journal on Scientific Computing*, 39(5):S88–S111, 2017.
- [31] O. Pironneau and D. F. Katz. Optimal swimming of flagellated microorganisms. *Journal of Fluid Mechanics*, 66(2):391–415, 1974.
- [32] M. Rumpf and O. Vantzos. Numerical gradient flow discretization of viscous thin films on curved geometries. *Mathematical Models and Methods in Applied Sciences*, 23(05), Feb. 2013.
- [33] J. Sokolowski and J.-P. Zolésio. *Introduction to Shape Optimization*. Springer Series in Computational Mathematics. Springer-Verlag, 1992.
- [34] W. Velte and P. Villaggio. On the detachment of an elastic body bonded to a rigid support. *Journal of Elasticity*, 27:133–142, 1992.
- [35] S. W. Walker. *The Shapes of Things: A Practical Guide to Differential Geometry and the Shape Derivative*, volume 28 of *Advances in Design and Control*. SIAM, 1st edition, 2015.
- [36] S. W. Walker. FELICITY: A Matlab/C++ toolbox for developing finite element methods and simulation modeling. *SIAM Journal on Scientific Computing*, 40(2):C234–C257, 2018.
- [37] O.-Y. Zhong-can and W. Helfrich. Bending energy of vesicle membranes: General expressions for the first, second, and third variation of the shape energy and applications to spheres and cylinders. *Phys. Rev. A*, 39(10):5280–5288, May 1989.